



**UNIVERSITI PUTRA MALAYSIA**

***OPTICAL, STRUCTURAL, THERMAL AND PHYSICAL PROPERTIES  
OF POLYMETHYLMETHACRYLATE AND POLYSULFONE  
NANOCOMPOSITES***

**RAOUF MAHMOOD RAOUF**

**FS 2016 3**



**OPTICAL, STRUCTURAL, THERMAL AND PHYSICAL PROPERTIES  
OF POLYMETHYLMETHACRYLATE AND POLYSULFONE  
NANOCOMPOSITES**

**By**

**RAOUF MAHMOOD RAOUF**

**Thesis Submitted to the School of Graduate Studies, Universiti Putra Malaysia,  
in Fulfillment of the Requirements for the Degree of Doctor of Philosophy**

**August 2016**

## COPYRIGHT

All material contained within the thesis, including without limitation text, logos, icons, photographs and all other artwork, is copyright material of Universiti Putra Malaysia unless otherwise stated. Use may be made of any material contained within the thesis for non-commercial purposes from the copyright holder. Commercial use of material may only be made with the express, prior, written permission of Universiti Putra Malaysia.

Copyright © Universiti Putra Malaysia



## DEDICATIONS

*To the spirit of my father Immaculate.....*

*My mother, Allah saves her.....*

*To my dear faithful wife*

*My children.*



Abstract of thesis presented to the Senate of Universiti Putra Malaysia in fulfillment of the requirement for the degree of Doctor of Philosophy

**OPTICAL, STRUCTURAL, THERMAL AND PHYSICAL PROPERTIES OF  
POLYMETHYLMETHACRYLATE AND POLYSULFONE  
NANOCOMPOSITES**

By

**RAOUF MAHMOOD RAOUF**

**August 2016**

**Chairman : Associate Professor Zaidan Abdul Wahab, PhD**  
**Faculty : Science**

Transparent polymers, such as polymethylmethacrylate (PMMA) and polysulfone (PSF), contain absorbing chromophores as a part of their structure. The chromophoric groups are able to absorb UV energy and involved in the photochemical degradation reactions leading to the formation of hydroperoxides and chain scission. Superb properties of environmentally friendly cellulose esters encourage us to use them as an inhibitor for photochemical interaction in addition to the high-formation ability. Moreover, the absorption peak of indium oxide nanoparticles (nano-In<sub>2</sub>O<sub>3</sub>) at round 280 nm. contribute to curb the photochemical interaction in the polymer matrix. The present thesis aims to improve PMMA and PSF in order to protect themselves and covered surfaces from the impact of UV radiation by using three environmentally friendly cellulose esters and the nano-In<sub>2</sub>O<sub>3</sub>. Two sets of transparent nano-composites based on PMMA and PSF were prepared separately with cellulose acetate butyrate (CAB), cellulose acetate propionate (CAP) and cellulose acetate phthalate (CAT) added with nano-In<sub>2</sub>O<sub>3</sub> using a twin screw extruder in various percentage concentrations.

The preparation process was divided into two stages; the first was preparing transparent samples from PMMA and PSF separately with CAB, CAP and CAT. The second was adding nano-In<sub>2</sub>O<sub>3</sub> to selected blend concentrations. Scans over UV and visible spectra for all highly transparent samples were made from 220 nm. to 800 nm. using a spectrophotometer. The results showed that the absorbance peak in the ultraviolet region for pure PMMA at 226 nm and for pure PSF at 268 nm, whilst the transmittance peak in the visible range for pure PMMA at 798 nm and for PSF at 712 nm. The results also showed that the increase in CAB, CAP and CAT percentage concentrations in blends reduce UV rays' absorbance while maintaining a high transmittance. The selection of specific concentrations PMMA/10%CAB, PMMA/10%CAP, PMMA/1%CAT, PSF/0.2%CAB, PSF/0.2% CAP and PSF/0.1% CAT represents less absorbance value within UV damage threshold for PMMA and PSF. The effect of nano-In<sub>2</sub>O<sub>3</sub> percentage concentrations on the absorbance and transmittance spectrum for PMMA and PSF was done using a spectrophotometer.

The results demonstrated that PMMA/0.05%/nano-In<sub>2</sub>O<sub>3</sub> and PSF/0.02%/nano-In<sub>2</sub>O<sub>3</sub> have maximum UV absorbance with high transmittance. Morphological and structural characterizations of selected samples were studied by means of Scanning Electron Microscopy (SEM) and Differential Scanning Calorimetry (DSC). The SEM results showed single phase for PMMA blends and composite surfaces, while PSF blends surfaces showed a size reduction in all blend and composite samples. The DSC results indicated that all samples are miscible. The thermogravimetry analysis (TGA) was used to characterize thermal behavior of the samples. The results indicated that pure PMMA degraded in three steps while pure PSF degraded in two steps. The TGA analyses also indicated that all CAB, CAP and CAT blends with PMMA and PSF have good thermal stability and adding nano-In<sub>2</sub>O<sub>3</sub> maintained the thermal stability for all samples. The dynamic mechanical Analysis (DMA) showed that the storage modulus and loss modulus of PMMA significantly increased by the incorporation of nano-In<sub>2</sub>O<sub>3</sub>. Finally, the samples PMMA/10% CAB/0.05% In<sub>2</sub>O<sub>3</sub> and PSF/0.2% CAP/0.02% In<sub>2</sub>O<sub>3</sub> are the best overall properties in this work.

Abstrak tesis yang dikemukakan kepada Senat Universiti Putra Malaysia sebagai memenuhi keperluan untuk ijazah Doktor Falsafah

**SIFAT OPTIK, STRUKTUR, TERMA DAN FIZIKAL  
POLYMETHYLMETHACRYLATE DAN POLYSULFONE**

Oleh

**RAOUF MAHMOOD RAOUF**

**Ogos 2016**

**Pengerusi : Profesor Madya Zaidan Abdul Wahab, PhD**  
**Fakulti : Sains**

Dua set komposit Nano lutsinar, yang berasaskan Polimetilmetakrilat (PMMA) dan polisulfon (PSF), mengandungi chromophores sebagai sebahagian daripada struktur mereka. Kumpulan-kumpulan chromophoric dapat menyerap tenaga UV dan terlibat dalam tindak balas fotokimia degradasi yang membawa kepada pembentukan hydroperoxides dan rantaian scission. Ciri-ciri luar biasa yang dimiliki oleh ester selulosa yang turut bersifat mesra alam menggalakkan kita untuk menggunakannya sebagai perencat bagi interaksi fotokimia sebagai tambahan kepada keupayaan-pembentukan tinggi. Selain itu, puncak penyerapan nanopartikel indium oksida (nano  $\text{In}_2\text{O}_3$ ) pada pusingan 280 nm. membendung interaksi fotokimia dalam matriks polimer. Kajian bertujuan untuk meningkatkan PMMA dan HPG sebagai langkah melindungi diri mereka dan permukaan dilindungi daripada kesan sinaran UV dengan menggunakan tiga ester selulosa mesra alam dan nano- $\text{In}_2\text{O}_3$ . Dua set komposit Nano lutsinar berdasarkan PMMA dan PSF telah disediakan secara bebas dengan selulosa asetat butyrate (CAB), selulosa asetat propionat (CAP) dan selulosa asetat phthalate (CAT) ditambah dengan nano  $\text{In}_2\text{O}_3$  menggunakan penitis skru berkembar dalam pelbagai peratusan kepekatan.

Proses penyediaan telah dibahagikan kepada dua peringkat; peringkat yang pertama ialah penyediaan sampel telus dari PMMA dan PSF berasingan dengan CAB, CAP dan CAT. Peringkat yang kedua ialah menambah nano  $\text{In}_2\text{O}_3$  kepada kepekatan campuran yang dipilih. Imbasan lebih UV dan spektrum yang boleh dilihat untuk semua sampel sangat telus dibuat daripada 220 nm. hingga 800 nm menggunakan spektrofotometer. Hasil kajian menunjukkan bahawa puncak keserapan di rantau ultraviolet untuk PMMA tulen adalah pada 226 nm. dan untuk PSF tulen adalah pada 268 nm, manakala puncak pemindahan dalam julat yang boleh dilihat untuk PMMA tulen ialah pada 798 nm dan untuk PSF ialah pada 712 nm. Keputusan juga menunjukkan bahawa peningkatan dalam kepekatan CAB, CAP dan peratusan CAT dalam campuran mengurangkan kuantiti sinar UV ' walaupun mengekalkan kadar pemindahan yang tinggi. Pemilihan kepekatan tertentu PMMA / 10% CAB, PMMA / 10% CAP, PMMA / 1% CAT, PSF /% CAB 0.2, PSF / 0.2% CAP dan PSF / 0.1%

CAT mewakili kurang nilai kuantiti dalam kerosakan UV ambang untuk PMMA dan PSF. Kesan kepekatan peratusan nano  $\text{In}_2\text{O}_3$  pada kuantiti dan pemindahan spektrum untuk PMMA dan PSF telah dilakukan dengan menggunakan spektrofotometer. Keputusan menunjukkan bahawa PMMA / 0.05% / nano  $\text{In}_2\text{O}_3$  dan PSF / 0.02% / nano  $\text{In}_2\text{O}_3$  mempunyai kuantiti UV maksimum dengan kadar pemindahan yang tinggi. Sampel akhir telah disediakan dari semua kepekatan. Morphological yang dipilih dan pencirian struktur sampel yang dipilih telah dikaji dengan cara menggunakan Scanning Electron Microscopy (SEM) dan Differential Scanning Calorimetry (DSC). Keputusan SEM menunjukkan fasa tunggal untuk campuran PMMA dan permukaan komposit, manakala PSF telah menggabungkan permukaan menunjukkan pengurangan saiz dalam semua gabungan dan sampel komposit. Keputusan DSC menunjukkan bahawa semua sampel terlarut boleh bercampur. Analisis termogravimetri (TGA) telah digunakan untuk mencirikan kelakuan terma sampel. Keputusan analisis menunjukkan bahawa PMMA tulen berkurangan dalam tiga langkah sementara PSF tulen berkurangan dalam dua langkah. TGA analisis juga menunjukkan bahawa semua CAB, CAP dan CAT campuran dengan PMMA dan PSF mempunyai kestabilan haba yang baik, terutamanya dengan menambah nano  $\text{In}_2\text{O}_3$  bagi mengekalkan kestabilan haba untuk semua sampel. Mekanikal Analisis dinamik (DMA) menunjukkan bahawa penyimpanan modulus dan kehilangan modulus PMMA meningkat dengan ketara. Secara keseluruhannya, sampel PMMA/10% CAB/0.05%  $\text{In}_2\text{O}_3$  dan PSF/0.2% CAP/0.02%  $\text{In}_2\text{O}_3$  menunjukkan sifat uvggul dalam projek ini.

## ACKNOWLEDGEMENTS

I would like to express my truthful gratefulness to Allah who gave me the ability, hope and patience to carry out this work. Allah, give me the power to thank you and worship you.

I wish to express my genuine thanks to my supervisor Assoc. Prof. Dr. Zaidan Abdul Wahab for his supervisions, guidance, supports and providing me with all necessary facilities. Also, I would like to give my truthful appreciation to Prof. Dr. Nor Azowa Ibrahim and Prof. Dr. Zainal Abidin Talib for their help, invaluable suggestions and counsels in order to keep me on the path during the research and Dr. Nizam Tamchek.

I am grateful to the Faculty of Science staff for their assistance during the period of the work.

This thesis was submitted to the Senate of Universiti Putra Malaysia and has been accepted as fulfillment of the requirement for the degree of Doctor of Philosophy. The members of the Supervisory Committee were as follows:

**Zaidan Abdul Wahab, PhD**  
Associate Professor  
Faculty of Science  
Universiti Putra Malaysia  
(Chairman)

**Zainal Abidin Talib, PhD**  
Professor  
Faculty of Science  
Universiti Putra Malaysia  
(Member)

**Nor Azowa Ibrahim, PhD**  
Associate Professor  
Faculty of Science  
Universiti Putra Malaysia  
(Member)

**Nizam Tamchek, PhD**  
Senior Lecturer  
Faculty of Science  
Universiti Putra Malaysia  
(Member)

---

**BUJANG BIN KIM HUAT, PhD**  
Professor and Dean  
School of Graduate Studies  
Universiti Putra Malaysia

Date:

## Declaration by graduate student

I hereby confirm that:

- this thesis is my original work;
- quotations, illustrations and citations have been duly referenced;
- this thesis has not been submitted previously or concurrently for any other degree at any other institutions;
- intellectual property from the thesis and copyright of thesis are fully-owned by Universiti Putra Malaysia, as according to the Universiti Putra Malaysia (Research) Rules 2012;
- written permission must be obtained from supervisor and the office of Deputy Vice-Chancellor (Research and Innovation) before thesis is published (in the form of written, printed or in electronic form) including books, journals, modules, proceedings, popular writings, seminar papers, manuscripts, posters, reports, lecture notes, learning modules or any other materials as stated in the Universiti Putra Malaysia (Research) Rules 2012;
- there is no plagiarism or data falsification/fabrication in the thesis, and scholarly integrity is upheld as according to the Universiti Putra Malaysia (Graduate Studies) Rules 2003 (Revision 2012-2013) and the Universiti Putra Malaysia (Research) Rules 2012. The thesis has undergone plagiarism detection software.

Signature: \_\_\_\_\_ Date: \_\_\_\_\_

Name and Matric No.: Raouf Mahmood Raouf (GS37764)  
\_\_\_\_\_

## TABLE OF CONTENTS

	<b>Page</b>
<b>ABSTRACT</b>	i
<b>ABSTRAK</b>	iii
<b>ACKNOWLEDGEMENTS</b>	v
<b>APPROVAL</b>	vi
<b>DECLARATION</b>	viii
<b>LIST OF TABLES</b>	xii
<b>LIST OF FIGURES</b>	xiii
<b>LIST OF ABBREVIATIONS</b>	xix
<b>LIST OF SYMBOLS</b>	xxi
<b>CHAPTER</b>	
<b>1 INTRODUCTION</b>	
1.1 Transparent Polymers	1
1.2 Thermal Behavior of Polymers	1
1.2.1 The Glass Transition Temperature (T <sub>g</sub> )	2
1.2.2 The Crystalline Melting Point (T <sub>m</sub> )	2
1.3 Polymer melt	3
1.4 Polymer blends and Copolymers	4
1.4.1 Polymer Blends	4
1.4.2 Copolymers	5
1.5 Composites	5
1.5.1 Composites Classification	5
1.6 Nanomaterials and Nanostructures	6
1.6.1 Nanomaterials Classification	7
1.7 Polymer nanocomposites	8
1.8 Polymer Degradation	8
1.9 Refractive Index	9
1.10 Problem Statement	10
1.11 Objectives	11
1.12 Thesis Layout	11
<b>2 LITERATURE REVIEW</b>	
2.1 Transparent Polymers, Preparation methods, blends and composites	12
2.1.1 Polymethylmethacrylate	12
2.1.2 Polysulfone	14
2.2 Bio-based polymers	16
2.2.1 Cellulose Esters	16
2.2.1.1 Cellulose Acetate Butyrate	17
2.2.1.2 Cellulose Acetate Propionate	20
2.2.1.3 Cellulose Acetate Phthalate	23
2.3 Nanoparticles and Nanocomposites	24
2.3.1 Indium Oxide Nanoparticles	24
2.3.2 Metal-Oxide Nanoparticle/Polymer Composites	25

<b>3</b>	<b>MATERIALS AND METHODOLOGY</b>	<b>31</b>
3.1	Introduction	31
3.2	Materials	31
3.3	Samples Preparation	31
3.4	Samples Characterization	35
3.5	UV-VIS Spectroscopy Measurements	36
3.6	Scanning Electron Microscopy	36
3.7	Thermogravimetric Analysis	37
3.8	Differential Scanning Calorimetry	37
3.9	Dynamic Mechanical Analysis	38
3.10	X-Ray Diffraction Measurements	38
3.11	Hardness Test	39
<b>4</b>	<b>RESULTS AND DISCUSSIONS</b>	<b>40</b>
4.1	Introduction	40
4.2	UV-VIS spectrophotometer analysis	40
4.2.1	Spectroscopy for PMMA and PSF blends	40
4.2.2	Spectroscopy of PMMA and PSF Nanocomposites	57
4.3	Morphological studies for Pure, Blend and Nanocomposite Samples	68
4.3.1	X-Ray Diffraction	68
4.3.2	Scanning Electron Microscope	73
4.5	Dynamic Mechanical Analysis	82
4.5.1	Dynamic mechanical properties of Pure PMMA, Blends and Nanocomposites	82
4.5.2	Dynamic mechanical properties of Pure PSF, Blends and Nanocomposites	85
4.6	Thermogravimetric Analysis	87
4.6.1	Thermogravimetric Analysis for pure PMMA, Blends and Nanocomposites	88
4.6.2	Thermogravimetric Analysis for pure PSF, Blends and Nanocomposites	92
4.7	Differential Scanning Calorimetry	102
4.8	Hardness	102
4.9	Refractive Index Determination	107
<b>5</b>	<b>CONCLUSION</b>	<b>116</b>
5.1	Summary of the Study	116
5.2	Conclusion	118
5.3	Prospects for Future Study	119
	<b>REFERENCES</b>	<b>120</b>
	<b>BIODATA OF STUDENT</b>	<b>136</b>
	<b>LIST OF PUBLICATIONS</b>	<b>137</b>

## LIST OF TABLES

<b>Table</b>		<b>Page</b>
3.1	Polymethylmethacrylate pure, blends and nanocomposite samples	33
3.2	Polysulfone pure, blends and nanocomposite samples	34
4.1	The crystalline peaks value at $2\theta$ and their corresponding Miller indices.	69
4.2	Glass Transition Temperatures ( $T_g$ ) for pure PMMA, blends and nanocomposites	85
4.3	Glass Transition Temperatures ( $T_g$ ) for pure PSF, blends and nanocomposites	87
4.4	The hardness value of pure PMMA, blends and nanocomposites	107
4.5	The hardness value of pure PSF, blends and nanocomposites	107
4.6	The value of energy gap and refractive index of pure PMMA and blends	114
4.7	The value of energy gap and refractive index for PMMA Bi-composite	114
4.8	The value of energy gap and refractive index for PMMA Tri-composite	114
4.9	The value of energy gap and refractive index of pure PSF and blends	115
4.10	The value of energy gap and refractive index for PSF Bi-composite	115
4.11	The value of energy gap and refractive index for PSF Tri-composite	115

## LIST OF FIGURES

Figure		Page
1.1	Diagram depicting morphology progress of the dispersed phases through melt mixing of immiscible polymers.	3
1.2	Common fiber reinforcement forms.	6
1.3	Schematic classification of nano – materials: (a) three – dimensional structures;(b) two – dimensional; (c) one – dimensional; and (d) zero – dimensional structures.	7
2.1	Polymethylmethacrylate structure	12
2.2	Polysulfone structure	14
2.3	Cellulose acetate butyrate structure	17
2.4	Cellulose acetate propionate structure	21
2.5	Cellulose acetate phthalate structure	23
2.6	Cubic indium oxide structure	24
3.1	Samples preparation scheme	35
3.2	X-ray diffraction scheme in a crystal material	39
4.1	PMMA/CAB absorbance and transmittance spectrum with concentration.	41
4.2	Absorbance of PMMA and CAB in different concentrations at 226 nm.	42
4.3	Transmittance of PMMA and CAB in different concentrations at 798 nm.	42
4.4	PMMA/CAB sheets in different concentrations.	43
4.5	PMMA/CAP absorbance and transmittance spectrum with concentrations.	44
4.6	Absorbance of PMMA and CAP in different concentrations at 226 nm.	45
4.7	Transmittance of PMMA and CAP in different concentrations at 798 nm.	45
4.8	PMMA/CAP sheets in different concentrations	46
4.9	PMMA/CAT absorbance and transmittance spectrum with concentrations	47
4.10	Absorbance of PMMA and CAT in different concentrations at 226 nm.	48

4.11	Transmittance of PMMA and CAT in different concentrations at 798 nm.	48
4.12	PMMA/CAT sheets in different concentrations	49
4.13	PSF/CAB absorbance and transmittance spectrum with concentrations	50
4.14	Absorbance of PSF and CAB in different concentrations at 268 nm.	51
4.15	Transmittance of PSF and CAB in different concentrations at 712.5 nm.	51
4.16	PSF/CAB sheets in different concentrations	52
4.17	PSF/CAP absorbance and transmittance spectrum with concentrations	52
4.18	Absorbance of PSF and CAP in different concentrations at 268 nm.	53
4.19	Transmittance of PSF and CAP in different concentrations at 712.5 nm.	53
4.20	PSF/CAP sheets in different concentrations	54
4.21	PSF/CAT absorbance and transmittance spectrum with concentrations	55
4.22	Absorbance of PSF and CAT in different concentrations at 268 nm.	56
4.23	Transmittance of PSF and CAT in different concentrations at 712.5 nm.	55
4.24	PSF/CAT sheets in different concentrations	57
4.25	The absorbance and transmittance spectrum for PMMA/nano-In <sub>2</sub> O <sub>3</sub>	59
4.26	The Absorbance of PMMA and nano-In <sub>2</sub> O <sub>3</sub> in different concentrations at 226 nm.	60
4.27	The Transmittance of PMMA and nano-In <sub>2</sub> O <sub>3</sub> in different concentrations at 798 nm.	60
4.28	PMMA/nano-In <sub>2</sub> O <sub>3</sub> sheets in different concentrations	61
4.29	The absorbance and transmittance spectrum for PSF/nano-In <sub>2</sub> O <sub>3</sub>	61
4.30	The Absorbance of PSF and nano-In <sub>2</sub> O <sub>3</sub> in different concentrations at 268 nm.	62
4.31	The Transmittance of PSF and nano-In <sub>2</sub> O <sub>3</sub> in different concentrations at 712.5 nm.	62

4.32	PSF/ nano-In <sub>2</sub> O <sub>3</sub> sheets in different concentrations	63
4.33	The absorbance and transmittance spectrum for pure PMMA, blends and nanocomposites	64
4.34	The absorbance values for pure PMMA, blends and nanocomposites	65
4.35	The transmittance values for pure PMMA, blends and nanocomposites	65
4.36	PMMA tri-composite sheets	66
4.37	The absorbance and transmittance spectrum for pure PSF, blends and nanocomposites	66
4.38	The absorbance values for pure PSF, blends and nanocomposites	67
4.39	The transmittance values for pure PSF, blends and nanocomposites	67
4.40	PSF tri-composite sheets	68
4.41	X-Ray diffractograms of powder nano-In <sub>2</sub> O <sub>3</sub> , powder CAB, pure PMMA, PMMA+nano-In <sub>2</sub> O <sub>3</sub> , PMMA+10% CAB and PMMA+10% CAB+0.05% nano-In <sub>2</sub> O <sub>3</sub>	69
4.42	X-Ray diffractograms of powder nano-In <sub>2</sub> O <sub>3</sub> , powder CAP, pure PMMA, PMMA+nano-In <sub>2</sub> O <sub>3</sub> , PMMA+10% CAP and PMMA+10% CAP+0.05% nano-In <sub>2</sub> O <sub>3</sub>	70
4.43	X-Ray diffractograms of powder nano-In <sub>2</sub> O <sub>3</sub> , powder CAT, pure PMMA, PMMA+nano-In <sub>2</sub> O <sub>3</sub> , PMMA+1% CAT and PMMA+1% CAT+0.05% nano-In <sub>2</sub> O <sub>3</sub>	70
4.44	X-Ray diffractograms of powder nano-In <sub>2</sub> O <sub>3</sub> , powder CAB, pure PSF, PSF+nano-In <sub>2</sub> O <sub>3</sub> , PSF+0.2% CAB and PSF+0.2% CAB+0.02% nano-In <sub>2</sub> O <sub>3</sub>	71
4.45	X-Ray diffractograms of powder nano-In <sub>2</sub> O <sub>3</sub> , powder CAP, pure PSF, PSF+nano-In <sub>2</sub> O <sub>3</sub> , PSF+0.2% CAP and PSF+0.2% CAP+0.02% nano-In <sub>2</sub> O <sub>3</sub>	72
4.46	X-Ray diffractograms of powder nano-In <sub>2</sub> O <sub>3</sub> , powder CAT, pure PSF, PSF+nano-In <sub>2</sub> O <sub>3</sub> , PSF+0.1% CAT and PSF+0.1% CAT+0.02% nano-In <sub>2</sub> O <sub>3</sub>	72
4.47	SEM images for pure PMMA and PMMA+0.05% nano-In <sub>2</sub> O <sub>3</sub> at three magnifications (2, 5, and 10 μm).	74
4.48	SEM images for PMMA+10% CAB and PMMA+10% CAB+0.05% nano-In <sub>2</sub> O <sub>3</sub> at three magnifications (2, 5, and 10 μm)	75

4.49	SEM images for PMMA+10%CAP and PMMA+10%CAP+0.05% nano-In <sub>2</sub> O <sub>3</sub> at three magnifications (2, 5, and 10 μm)	76
4.50	SEM images for PMMA+1%CAT and PMMA+1%CAT+0.05% nano-In <sub>2</sub> O <sub>3</sub> at three magnifications (2, 5, and 10 μm)	77
4.51	SEM images for pure PSF and PSF+0.02% nano-In <sub>2</sub> O <sub>3</sub> at three magnifications (2, 5, and 10 μm)	78
4.52	SEM images for PSF+0.2% CAB and PSF+0.2% CAB+0.02% nano-In <sub>2</sub> O <sub>3</sub> at three magnifications (2, 5, and 10 μm)	79
4.53	SEM images for PSF+0.2%CAP and PSF+0.2%CAP+0.02% nano-In <sub>2</sub> O <sub>3</sub> at three magnifications (2, 5, and 10 μm)	80
4.54	SEM images for PSF+0.1%CAT and PSF+0.1%CAT+0.02% nano-In <sub>2</sub> O <sub>3</sub> at three magnifications (2, 5, and 10 μm)	81
4.55	Storage modulus variation with temperature for pure PMMA, blends and nanocomposites	83
4.56	Loss modulus variation with temperature for pure PMMA, blends and nanocomposites	84
4.57	Loss factor variation with temperature for pure PMMA, blends and nanocomposites	84
4.58	Storage modulus variation with temperature for pure PSF, blends and nanocomposites	86
4.59	Loss modulus variation with temperature for pure PSF, blends and nanocomposites	86
4.60	Loss factor variation with temperature for pure PSF, blends and nanocomposites	87
4.61	The TGA and DTG curves for pure PMMA	89
4.62	The TGA and DTG curves for PMMA+10% CAB	90
4.63	The TGA and DTG curves for PMMA+10% CAP	91
4.64	The TGA and DTG curves for PMMA+1% CAT	91
4.65	The TGA and DTG curves for PMMA+0.05% nano-In <sub>2</sub> O <sub>3</sub>	92
4.66	The TGA and DTG curves for PMMA+10% CAB+0.05% nano-In <sub>2</sub> O <sub>3</sub>	93
4.67	The TGA and DTG curves for PMMA+10% CAP+0.05% nano-In <sub>2</sub> O <sub>3</sub>	94

4.68	The TGA and DTG curves for PMMA+1% CAT+0.05% nano-In <sub>2</sub> O <sub>3</sub>	95
4.69	The TGA and DTG curves for pure PSF	96
4.70	The TGA and DTG curves for PSF+0.2% CAB	97
4.71	The TGA and DTG curves for PSF+0.2% CAP	97
4.72	The TGA and DTG curves for PSF+0.1% CAT	98
4.73	The TGA and DTG curves for PSF+0.02% nano-In <sub>2</sub> O <sub>3</sub>	99
4.74	The TGA and DTG curves for PSF+0.2% CAB+0.02% nano-In <sub>2</sub> O <sub>3</sub>	100
4.75	The TGA and DTG curves for PSF+0.2% CAP+0.02% nano-In <sub>2</sub> O <sub>3</sub>	101
4.76	The TGA and DTG curves for PSF+0.1% CAT+0.02% nano-In <sub>2</sub> O <sub>3</sub>	101
4.77	DSC curves of pure PMMA, PMMA+10% CAB, PMMA+10% CAP and PMMA+1% CAT	103
4.78	DSC curves of PMMA+0.05% nano-In <sub>2</sub> O <sub>3</sub> , PMMA+10% CAB+0.05% nano-In <sub>2</sub> O <sub>3</sub> , PMMA+10% CAP+0.05% nano-In <sub>2</sub> O <sub>3</sub> and PMMA+1% CAT+0.05% nano-In <sub>2</sub> O <sub>3</sub>	104
4.79	DSC curves of pure PSF, PSF+0.2% CAB, PSF+0.2% CAP and PSF+0.1% CAT	105
4.80	DSC curves of PSF+0.02% nano-In <sub>2</sub> O <sub>3</sub> , PSF+0.2% CAB+0.02% nano-In <sub>2</sub> O <sub>3</sub> , PSF+0.2% CAP+0.02% nano-In <sub>2</sub> O <sub>3</sub> and PSF+0.1% CAT+0.02% nano-In <sub>2</sub> O <sub>3</sub>	106
4.81	Variation of $(\alpha h\nu)^2$ as a function of photon energy $h\nu$ for pure PMMA, PMMA+5% CAB, PMMA+7% CAB, PMMA+8% CAB and PMMA+9% CAB	108
4.82	Variation of $(\alpha h\nu)^2$ as a function of photon energy $h\nu$ for PMMA+10% CAB, PMMA+11% CAB, PMMA+13% CAB, PMMA+15% CAB, PMMA+20% CAB and PMMA+25% CAB	108
4.83	Variation of $(\alpha h\nu)^2$ as a function of photon energy $h\nu$ for pure PMMA, PMMA+5% CAP, PMMA+7% CAP, PMMA+9% CAP, PMMA+10% CAP	109
4.84	Variation of $(\alpha h\nu)^2$ as a function of photon energy $h\nu$ for PMMA+11% CAP, PMMA+13% CAP, PMMA+15% CAP and PMMA+20% CAP	109

4.85	Variation of $(\alpha h\nu)^2$ as a function of photon energy $h\nu$ for pure PMMA, PMMA+1%CAT, PMMA+2%CAT, PMMA+3%CAT, PMMA+4%CAT and PMMA+5%CAT	110
4.86	Variation of $(\alpha h\nu)^2$ as a function of photon energy $h\nu$ for pure PMMA, PMMA+ 0.01% nano-In <sub>2</sub> O <sub>3</sub> , PMMA+ 0.02% nano-In <sub>2</sub> O <sub>3</sub> , PMMA+ 0.03% nano-In <sub>2</sub> O <sub>3</sub> , PMMA+ 0.04% nano-In <sub>2</sub> O <sub>3</sub> and PMMA+ 0.05% nano-In <sub>2</sub> O <sub>3</sub>	110
4.87	Variation of $(\alpha h\nu)^2$ as a function of photon energy $h\nu$ for PMMA+10% CAB 0.02% nano-In <sub>2</sub> O <sub>3</sub> , PMMA+10% CAP+ 0.02% nano-In <sub>2</sub> O <sub>3</sub> and PMMA+1%CAT+ 0.02% nano-In <sub>2</sub> O <sub>3</sub>	111
4.88	Variation of $(\alpha h\nu)^2$ as a function of photon energy $h\nu$ for pure PSF, PSF+0.1% CAB, PSF+0.2% CAB, PSF+0.3% CAB and PSF+0.4% CAB	111
4.89	Variation of $(\alpha h\nu)^2$ as a function of photon energy $h\nu$ for pure PSF, PSF+0.1% CAP, PSF+0.2% CAP, PSF+0.3% CAP and PSF+0.4% CAP	112
4.90	Variation of $(\alpha h\nu)^2$ as a function of photon energy $h\nu$ for pure PSF, PSF+0.1% CAT, PSF+0.2% CAT, PSF+0.3% CAT and PSF+0.4% CAT	112
4.91	Variation of $(\alpha h\nu)^2$ as a function of photon energy $h\nu$ for pure PSF, PSF+0.1% CAT, PSF+0.2% CAT, PSF+0.3% CAT and PSF+0.4% CAT	113
4.92	Variation of $(\alpha h\nu)^2$ as a function of photon energy $h\nu$ for PSF+0.2% CAB+0.02% nano-In <sub>2</sub> O <sub>3</sub> , PSF+0.2% CAP+0.02% nano-In <sub>2</sub> O <sub>3</sub> and PSF+0.1% CAT+0.02% nano-In <sub>2</sub> O <sub>3</sub>	113

## LIST OF ABBREVIATIONS

AFM	Atomic force microscopy
ATR-RTIR	Attenuated total reflection-Fourier transform infrared spectroscopy
BAM	Brewster angle microscopy
CCMC	Carbon-matrix composites
CAB	Cellulose acetate butyrate
CAT	Cellulose acetate phthalate
CAP	Cellulose acetate propionate
CMC	Ceramic-matrix composites
CDS	Chemical solution decomposition
DSC	Differential scanning calorimetry
DTA	Differential thermal analysis
DMF	dimethylformamide
DLS	Dynamic light scattering
DMA	Dynamic mechanical analysis
DMTA	Dynamic mechanical thermal analysis
LCR	Electronic test equipment
FESEM	field emission scanning electron microscopy analyses
FTIR	Fourier Transform Infrared Spectroscopy
GPC	Gel permeation chromatography
HRTEM	High resolution transmission electron microscopy
MMC	Metal-matrix composites
MW	Molecular weight
NCP	Nanocomposites
NM	Nanomaterials
NPS	Nanoparticles
NIR	Near infrared
NMR	Nuclear magnetic resonance spectroscopy
OLS	Okazaki large spectrograph
OMC	Organic-matrix composites

PL	Photoluminescence
PC	Polycarbonate
PDLC	Polymer dispersed liquid crystals
PNC	Polymer nanocomposites
PMCs	Polymer-matrix composites
PMMA	Polymethylmethacrylate
PSF	Polysulfone
RAFT	Reversible addition fragmentation chain transfer
SEM	Scanning electron microscope
STEM	Scanning transmission electron microscope
SEC	Size exclusion chromatography
SCT	Solution cast technique
SCM	Spin coating method
TG-DTA	Thermogravimetric differential thermal analysis
XRF	X-ray fluorescence
UVC	Ultraviolet range (100-280)
UV-VIS-IR	Ultraviolet-visible-near infrared spectrophotometer
WXR	Wide-angle X-ray diffraction

## LIST OF SYMBOLS

$A$	Absorbance of the same absorbed beam
$Ca$	Capillary number
$\Delta H_m$	Enthalpy change during melting
$\Delta S_m$	Entropy change during melting
$T_g$	Glass Transition Temperature
$\alpha_e$	Molar absorption coefficient.
$X_i$	Number of molecules
$I$	The absorbed intensity of the same beam
$\theta$	The angle between incident beam and planes
$R$	The droplet radius
$\Delta C_p$	The heat capacity
$\lambda$	The incident beam wavelength
$I_0$	The beam intensity of special wavelength
$\tau$	The ratio of the shear stress
$C$	The sample concentration
$\dot{\gamma}$	The shear rate
$\gamma$	The surface tension
$w$	The weight fraction
$\rho$	Viscosity ratio
$\eta_d$	Viscosity for the dispersed phase
$\eta_m$	Viscosity of the matrix
$\bar{M}_w$	Weight average molecular weight

# CHAPTER 1

## INTRODUCTION

### 1.1 Transparent Polymers

In a world full of different types of polymers it is perhaps the transparent ones that give the greatest benefit to our lives because it is involved in numerous applications (from eye glasses to solar concentrating lenses for spacecraft power and propulsion systems) (Edwards et al., 2000). It has now become indispensable in all areas of life. The structure of transparent polymers does not differ significantly from non-transparent (opaque) polymers, that only transparent polymers are often amorphous and the blends mostly miscible. There are about 120 types of transparent polymers most of them are acrylic with transmittance more than 90% and refractive index of 1.5-1.6. Polysulfone as one of transparent polymers that has a refractive index 1.63 and transmittance of about 80% (Seymour and Carraher, 1984). The most common transparent polymer is PMMA and polycarbonate (PC). In order to apply polymers in optical uses, they must have different refractive indices (Prasad, 2012). As a result of their functional performance polymers transparency is affected by UV radiation and weather conditions leading to a decrease in transparency (photolysis) because of oxidative degradation that lead to molecular chain scission (Hamdy et al, 2016; Sun et al., 2016).

### 1.2 Thermal Behavior of Polymers

The thermal transitions in polymers are slightly different and more complex than non-organic. First, the molecules are large enough to be suitably called polymers and do not exist in the gaseous state and they decompose rather than boil. Second, polymer consists of a mixture of molecules possessing different chain lengths (different molecular weights), so the transition from solid to liquid form of a polymer is rather diffuse and occurs over a temperature range between 2 and 10 °C depends on the polydispersity of the polymer. Third, the polymers become very viscous fluids (viscoelastic form) in the melting.

The molecular motion in a polymer is promoted by its thermal energy and opposed by the cohesive forces between structural pieces along the chain in addition to neighboring chains. These cohesive forces and, as a result, thermal transitions in polymers rely on polymer structure. In this regard, Polymeric materials are characterized by two major types of transition temperatures, the glass transition temperature ( $T_g$ ) and the crystalline melting temperature ( $T_m$ ).

The transition from the hard (brittle glass) to a softer (rubbery) state in amorphous polymers occurs through a temperature range called the glass transition temperature ( $T_g$ ) and in the case of a partially crystalline polymer the transformation occurs only in the amorphous regions whilst the crystalline zones remain unchanged and act as reinforcing elements so the polymer be hard and tough. If heating is continued, the polymer crystalline zones initiate melting. The equilibrium crystalline melting point

( $T_m$ ) for polymers will be the temperature at which the last crystalline starts melting. It is noteworthy that the value of ( $T_m$ ) depends on the degree of crystallinity and size distribution of crystallites (Ebewele, 2000; Odian, 2004).

### **1.2.1 The Glass Transition Temperature ( $T_g$ )**

The glass transition temperature term observes in linear amorphous polymers, such as poly methylmethacrylate or polystyrene. It occurs at well-known temperatures. When the bulk material is heated to temperatures above the glass transition temperature ( $T_g$ ) turns from brittle and glassy to soften like rubber or liquefy depending on their degree of cross-linking and/or molecular weight. In the case of semi crystalline materials (polypropylene, polyethylene)  $T_g$  is much lower than melting point and represents the temperature range in which on cooling the brittleness increases noticeably (Rieger, 2001).

Many physical properties like mechanical damping, heat capacity, coefficient of thermal expansion, electrical properties and refractive index change profoundly at  $T_g$  because they depend on the relative degree of freedom of molecular motion within polymeric materials and each property can be used to monitor the point at which  $T_g$  occurs (Nicholson, 2012; Rieger, 2001). The rheological definition of glass transition is that the glass transition occurs when the viscosity is  $10^{12}$  Pa.s.

The  $T_g$  depends on the cooling rate because glass transition is kinetic property. When the cooling rate (normal cooling rate in glass studies 10K/min) increases, glass transition would occur at a high temperature; when the cooling rate decreases, glass transition would occur at low temperature (Zhang, 2008).

The most common methods for determining the glass transition temperature are Differential Thermal Analysis (DTA), Differential Scanning Calorimetry (DSC) and Dynamic Mechanical Analysis (DMA) (Rieger, 2001).

### **1.2.2 The Crystalline Melting Point ( $T_m$ )**

Melting includes a change from the crystalline solid state to the liquid form. For low molecular weight materials, melting represents a first order thermodynamic transition characterized by discontinuities in the primary thermodynamic factors of the material system such as specific volume (density), heat capacity, transparency and refractive index. Melting happens when the change in free energy of the process is zero.

The crystalline polymers do not have clear melting points. This is because they are effectively mixtures, including components from a range of relative molar masses, each component of which melt at different temperature. Thus, low relative molar mass homopolymers melt at lower temperatures than high relative molar mass species. The size of the crystallites also influences the range of the melting temperature, as smaller and less perfect crystallites melt before large ones when the temperatures are heating up.

There are two other factors which influence the value of the temperature range over which melting takes place:

- First is the presence of co-monomer in the polymer, involving copolymerization, this factor reducing the melting point by shortening the crystallisable series length within the individual polymer molecules.
- Second is the presence of solvent trace or solvent plasticizer in the polymer, this factor dose so by increasing the relative mobility of the polymer molecules in the material, so reducing the necessary energy to take them into the liquid phase (Nicholson, 2012).

### 1.3 Polymer melt

Polymers can be illustrious by their properties, especially the change that occurs after heating, which relates to their change in stiffness and damping. Each polymer has individual physical properties that will set their use in practice. It is important to be able to determine the nature of an unknown polymer for many reasons. The first is to be able to determine the quality and dependability of a manufacturing process, to see that the final product is of a steady composition with time. The second is to match up polymers from different origins, of apparently similar groups. Finally, it is often important to be able to determine the nature of a plastic of unknown origin (Faria et al., 2007).

The melt blending is a complex procedure which includes melting of pellets, dispersive mixing, distributive mixing, and droplet cohesion. Dispersive mixing is a procedure in which the size of a dispersed phase decreases because of applied stresses, even as distributive mixing includes homogenization of the dispersed phase inside a matrix. Figure 1.2 shows how dispersed phase morphology creates throughout melt compounding. At first, pellets of the minor component melt and a thin film of the dispersed phase is structured on the surfaces of the mixing equipment because of shear forces. This film is precarious and creates holes as a consequence of interfacial unsteadiness, structuring a lace-like formation of thin filaments which at last separation into droplets. Without a compatibilizer at the phase interface a coarser morphology is formed because of droplets cohesion of, whilst a better dispersion is gotten with a compatibilizer (Cheerarot, 2012; Ryan, 1998; Scott and Macosko, 1995).

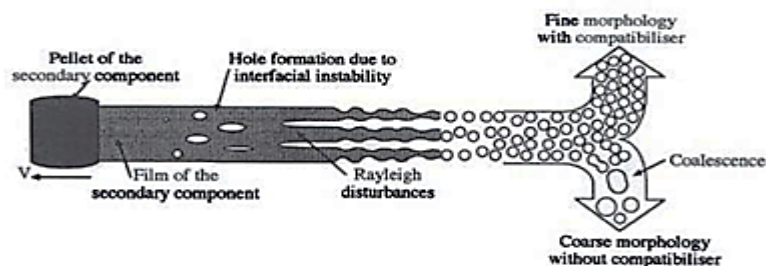


**Figure 1.1: Diagram depicting morphology progress of the dispersed phases through melt mixing of immiscible polymers (Ryan, 1998).**

## 1.4 Polymer Blends and Copolymers

### 1.4.1 Polymer Blends

Polymer blends are physical mixtures of two or more polymers (these polymers could be homopolymers or copolymers). It has been estimated that ~ 30% of all polymers are solid in mixed form. Attention on these materials has been increased firstly from the ability to develop mechanical properties. The phase behavior of polymer blend systems is a function of temperature, pressure and concentration. The huge majority of polymer blends has been found to be multiphase - either completely immiscible or multiphase with some limited mixing. This is mostly the result of the small combinatorial entropy of blending for the disparate polymer chains. The remaining part is a single phase, melt-miscible mixtures (Cheng, 2002; Ibrahim and Kadum, 2010).

Polymer blends consist of 30 – 40% of polymer products, and gradually more employed in the new materials design. Among the reasons that led to blends to be of considerable interest are:

- Adaptability in detail end product properties.
- Synergistic arrangements of blend ingredients to optimize the properties, such as improving mechanical, optical, thermal and electrical properties.
- Low investment cost of novel materials design and low cost.

Most profitable blends consist of two polymers and a small amount of a third compatibilizing polymer (typically copolymer). Polymer blends are combination of independent molecular distributions, which can vary in molecular weight MW and structure of functional groups.

Several techniques have been utilized to distinguish single and multi-phase character in polymer blends. Optical clarity is frequently used as a first indication, in the absence of crystallinity; a single-phase material is expected to be optically clear while a multi-phase mixture should be opaque. Optical and electron microscopy techniques are used often in an attempt to find out phase structure in polymer blends and block copolymers. The dependence on the atomic force microscopy (AFM) will help to characterize the phase-separated structure of phase separated blends and copolymers. Measurement of the location and number of T<sub>g</sub> by thermal analysis techniques is the most common approach to evaluate phase behavior in a particular temperature range in polymer blends. In a binary mixture, if two T<sub>g</sub>'s are observed at the same temperatures as those of the component polymers, means that the polymers are completely immiscible. A single T<sub>g</sub> between the components indicates miscibility. The intervals of T<sub>g</sub> in miscible polymers are frequently broadened compared to those of the components, as a result of a distribution of local surroundings. There is also two T<sub>g</sub>'s but shifted inwards from the components. This is generally taken to indicate multiphase behavior with some mixing between the components. A partially miscible blend as well can happen in polymer blends (Cheng, 2002; Ibrahim and Kadum, 2010).

Many expressions have been used to predict T<sub>g</sub> of miscible mixtures. The Fox-Flory equation, primarily derived for random copolymers, is probably the most widely used (Cheng, 2002; Ibrahim and Kadum, 2010).

Attempts have also been made to connect the experimentally derived (T<sub>g</sub>)s of miscible blends to intermolecular interactions (Ibrahim and Kadum, 2010; Kwei et al., 1987; Lu and Weiss, 1992).

### 1.4.2 Copolymers

Copolymers are macromolecules that are created from two or more different monomer units. The basic arrangements of the building blocks are determined by relative monomer reactivities and the synthetic procedures used. Different chemical units can be arranged in random, blocky or alternating fashion. The most common block copolymers are: diblocks (where relatively long segments of monomers A and B are connected at one end); triblock copolymers (the An-Bin-An type); and multiblock copolymers ( $[A-A \dots A-B-B \dots B]_x$ ). The alternating and random copolymers frequently show a single phase structure, conversely high molecular weight (block and graft copolymers) often exhibits phase separated morphology. However, microphase separation can watch, because of the interconnectivity of the kinds, as opposed to separation of large scale, that found in the great bulk of polymer blends.

Thermoplastic elastomers are an important class of materials that are frequently derived from tri or multi-block arrangements. These polymers are consisting of a comparatively high concentration of soft (molecule) (blocks that are amorphous and have low T<sub>g</sub>) besides two or more hard (molecule). The hard molecules provide physical crosslinks (reinforcement) and are either amorphous with T<sub>g</sub> > room temperature or crystalline with a melting point above room temperature (Styrene-butadiene-styrene triblock copolymers) (Cheng, 2002).

## 1.5 Composites

A composite material is a macroscopic combination of two or more different materials, having detectible interface between them. Composites are used in electrical, thermal, structural properties and environmental applications. Current composite materials are ordinarily optimized to get a particular balance of properties for a given range of applications. Therefore, composites normally have a fiber or particle that is stronger and stiffer than the continuous matrix phase. Different types of reinforcements as well have good thermal and electrical conductivity.

### 1.5.1 Composites Classification

Generally, composites are classified in two different levels:

- The first level is usually based on the matrix ingredient. The main composite is comprised of organic-matrix composites (OMCs), ceramic-matrix

composites (CMCs) and metal-matrix composites (MMCs). Normally, OMCs supposed to include two classes of composites: polymer-matrix composites (PMCs) and carbon-matrix composites (CCMC) (typically referred to as carbon-carbon composites). Commonly, CCMC are formed from PMCs by involving the extra steps of carbonizing and condensation the original polymer matrix.

- The second level is based on the reinforcement from particulate reinforcements, continuous fiber laminated composites, whisker reinforcements and woven composites as shown in Figure 1.2 (Zweben, 1998). Generally, the substantial volume fraction of the reinforcement is about ~10% or more to provide a useful increase in properties. Thus, particulate reinforced composites include those reinforced by spheres, flakes, rods and many other forms of approximately equal axes. The whisker reinforcements, with an aspect ratio typically between 20 and 100, are often considered together with particulates in MMCs. Mutually, these are sorted as a discontinuous reinforcements, because the reinforcing phase is intermittent for the lower volume fractions typically used in MMCs. While continuous fiber reinforced composites include reinforcements having lengths much bigger than their cross sectional dimensions and a large amount of them include fibers that are similar in size (length) to a general dimensions of the composite part. Each layer of a continuous fiber composite usually has a specific fiber orientation direction as in Figure 1.3.

There is also filled structure. The filler particles are included for the purpose of cost decrease more willingly than reinforcement, these composites, generally, not considered as a particulate composite (Miracle and Donaldson, 2003; Zweben, 1998).

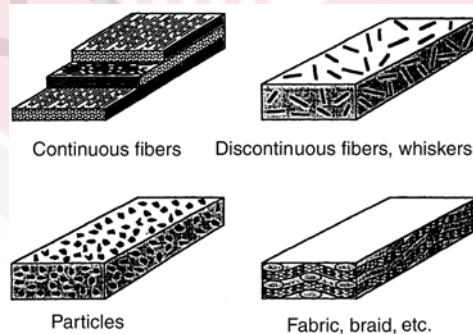


**Figure 1.2: Common fiber reinforcement forms (Zweben, 1998).**

## 1.6 Nanomaterials and Nanostructures

Nanomaterials (NM) are generally regarded as materials with a minimum of external dimension that measures less than 100 nm. or with internal structures measuring not as much of 100 nm. They possibly will be in the form of particles, tubes, rods or fibers. The nanomaterials that have the similar composition as known bulk form materials possibly will have different physic-chemical properties than the similar materials in bulk form, and may act in a different way if they enter the body.

### 1.6.1 Nanomaterials Classification

The production of materials and devices with new properties by method of controlling their microstructure on the atomic level has turned into a rising interdisciplinary field comprising of solid state physics, biology, chemistry and material science. The materials and devices included could be classified into the following three groups: The first group includes materials and devices with reduced dimensions in the shape of isolated, substrate-supported or embedded nanometer extent particles, thin wires or thin films. The second group includes materials and devices in which the nanometer extent microstructure is limited to a thin surface area of a bulk material, and the third category of bulk solids with a nanometer extent microstructure (Gleiter, 2000; Zweben, 1998).

One of the essential consequences of the materials science is the knowledge that most properties of solids rely on the microstructure. A decrease in the spatial dimension, or imprisonment of particles or semi-particles in a specific crystallographic direction inside the structure normally leads to changes in physical properties of the system in that direction. Therefore an additional classification of nanostructured materials and systems basically relies on the number of dimensions which exist within the nanometer range: zero dimensional structures, like nano-pores and nano-particles, one dimension, possessing only one dimension in the nanometer scale, and thus are as lamellae. Graphene and clays are known as being nano-layered particles. Two dimensions, the particles have two dimensions in the nanometer range and the third dimension is larger, their structure is extended. Cellulose nano-whiskers and carbon nanotubes are typical examples of this group. Three dimensions, when the particles have three nanoscale dimensions they are named ISO dimensional nanoparticles like spherical silica nanoparticles Figure 1.4 (Cheerarot, 2012; Pokropivny, 2007):

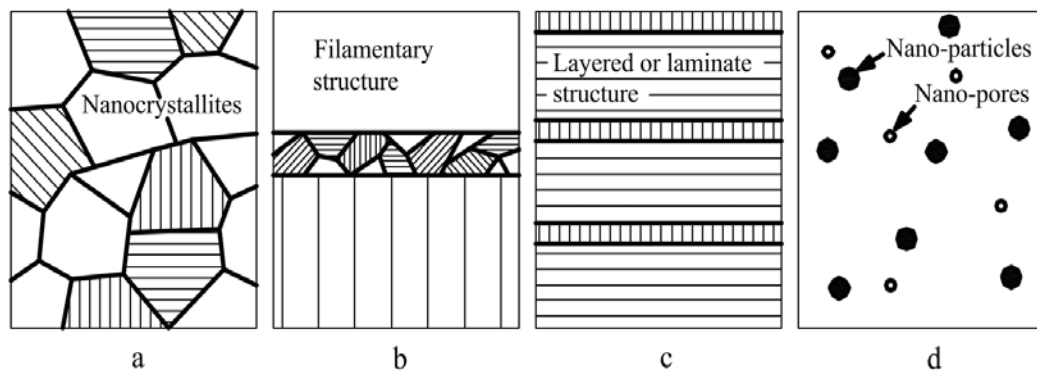


**Figure 1.3: Schematic classification of nano – materials: (a) three – dimensional structures;(b) two – dimensional; (c) one – dimensional; and (d) zero – dimensional structures (Pokropivny, 2007).**

## 1.7 Polymer nanocomposites

Polymer nanocomposite (PNC) is a mixture of composites and nano-sized materials, it consists of two types of materials, a host polymer and nano-size filler. Polymer based nano composite is getting an increasing interest because of substantial enhancements in the physical and chemical properties of the materials. The logic behind these properties enhancement is the small size of fillers and homogeneous dispersion on the nano-scale within a polymer matrix in addition to the length scale of interaction with the polymer segments. There is a high volume fraction of an interface area between the polymer matrix and the nanoparticles because of the small particle size (Vaia and Giannelis, 2001). Therefore, a small amount of nano-filler can improve the polymer properties by several orders of magnitude. Also, the molecular mobility and packing density of the segments in that interface quite different from those in the matrix polymer (Kotsilkova et al., 2005). A few methods have been utilized to describe the structure and properties of PNCs like, X-ray diffraction (XRD), Scanning Electron Microscope (SEM), Fourier Transform Infrared Spectroscopy (FTIR) and transmission electron microscopy (TEM) (Chen et al., 2009; Olmos et al., 2014).

## 1.8 Polymer Degradation

The ultraviolet region in optical spectrum is the most harmful part of sunlight owing to its high energy. The photon energy related to it is of the order (from 0.3 to 0.4 MJ) , which is in the range of C—C energy, ultraviolet radiation could cause C—C bonds break, ensuing a scission of the polymer chain. Other bonds like C—O and C—H might also break. PMMA absorbs up to 95% of the incident UV rays within the range of UVC 100–280. The most important feature of arbitrary scission in a polymer chain is a fast decrease in the MW. The changes that happen in the physical properties of a polymer in addition to MW leads to decrease in its mechanical properties and its ability to perform satisfactorily in a few applications (Abouelezz and Waters 1978, Mitsuoka et al., 1993; Yousif et al. 2015). The arbitrary scission leads to the disintegration of the chemical bond to generate free-radical. There may be more than one free-root in a composition (Abouelezz and Waters, 1978; Rabek and Fouassier, 1989).

In PMMA, the number of scissions occurring in its chains relative to the number of quanta that absorbed by the chain and they recognized the proportionality constant as the quantum yield of chain scission (Abouelezz and Waters, 1978).

It was found that at room temperature random main chain fracture in PMMA degradation happens with ultra-violet UV radiation, while at higher temperatures the reaction is one of chain depolymerization. The energy amount that absorbed for each main chain fracture is about 550 eV with ultraviolet radiation, so that less than 1% of the quanta absorbed are effectual. In recent times, the wavelength sensitivity in photodegradation of PMMA was studied by monochromatic radiation using the Okazaki Large Spectrograph (OLS). It was discovered that the limit wavelength of main chain scission is between 260-320 nm.

Furthermore, the number of main-chain scission which has a greater value in the case of the irradiation with 280 nm. (Mitsuoka et al., 1993; Torikai and Hasegawa, 1998; Torikai et al., 1990).

## 1.9 Refractive Index

The refractive index ( $n$ ) of the medium is a number describing how fast the light travels through a specific medium relative to light speed in vacuum. Generally, the refractive index defined by:

$$n = \frac{c}{v} \quad (1.1)$$

where  $c$  is the light speed in a vacuum, and  $v$  is the light speed in the medium.

The refractive index used as a measure of the material purity and optical design. In the field of transparent polymers, studying refractive index of the material gives a clear picture of the behavior of the penetrating rays in the material. The refractive index of the homogeneous material is isotropic even the molecules are oriented randomly (Kuzyk, 2006).

Practically, the refractive index measured directly by refractometer. Theoretically, it can find out from the optical band gap which obtained from the absorption curve edge of UV-VIS spectra. The absorption coefficient  $\alpha$  can find from absorbance value  $A = \log \frac{I_0}{I}$  using the relation (Asha et al., 2009):

$$\alpha(h\nu) = 2.303A/T \quad (1.2)$$

where  $T$  is the thickness of the sample,  $I_0$  is the intensity of the incident beam and  $I$  is the intensity of the incident beam. The optical band gap determined from the curve tangent in the absorption edge for  $(\alpha h\nu)$  against  $(h\nu)$ . The empirical relation between the optical band gap and refractive index proposed for different compounds by Reddy (Reddy et al., 1998):

$$n = \sqrt[2]{\frac{12.417}{Eg - 0.365}} \quad (1.3)$$

where Reddy equation is the modified form of Moss equation which proposed that the energy levels in a solid material are scaled down by the factor  $1/n^4$ . The Reddy equation compatible with practical results than Moss equation (Kumar and Singh, 2010).

## 1.10 Problem Statement

One of the major problems experienced in transparent polymers is degradation emerging from its exposure to sunlight (Ultraviolet radiation), which leads to changes in material color, surface glimmering and the cracks appearance of a surface. As a result, reduces the lifetime of the product. This issue up to some transparent polymers, such as PMMA and PSF, contain strongly absorbing chromophores as an integral part of their structure. The chromophores are capable to absorb UV ray energy and involve in the photochemical degradation reactions that occur via free radical mechanisms, leading to the formation of hydroperoxides and chain scission of the polymer. There are many researches which are based on blending the polymer as a solution of its problems. So choosing to blend PMMA and PSF with UV inhibitors in order to minimize photochemical interaction.

Unusual optical and thermal properties of eco-friendly cellulose esters motivate us to use them as an inhibitor for photochemical interaction in addition to the high-formation ability. Moreover, indium oxide nanoparticles (nano-In<sub>2</sub>O<sub>3</sub>) show a strong absorption below 450 nm with an absorbance peak at round 288 nm, it may contribute to curb the photochemical interaction with the polymer matrix (Maensiri et al., 2008a).

## 1.11 Objectives

The goal of the present thesis is to improve two important transparent polymers (Polymethylmethacrylate-PMMA and Polysulfone-PSF) in order to protect themselves and covered surfaces from the impact of ultraviolet radiation by using some environmentally friendly cellulose esters with nanomaterial. The objectives of this thesis:

1. To study the effect of adding different percentage concentrations of cellulose acetate derivatives (cellulose acetate butyrate CAB - cellulose acetate propionate CAP - cellulose acetate phthalate CAT) on absorbance and transmittance spectrum of PMMA and PSF blends separately in order to select less absorbency within ultraviolet region and high transmittance in the visible region, with taking into consideration the transparency of samples.
2. To analyze bi-composite samples PMMA/nano-In<sub>2</sub>O<sub>3</sub> and PSF/nano-In<sub>2</sub>O<sub>3</sub> using UV-VIS spectrum and select maximum absorbance. Then, formulate tri-composite samples which consist of selected PMMA/cellulose acetate derivatives and PSF/cellulose acetate derivatives individually with the addition of the selected concentrations of nano-In<sub>2</sub>O<sub>3</sub>.
3. To study the morphology of all selected samples beside pure PMMA and pure PSF in addition to study the mechanical, thermal and thermo-mechanical properties of all selected samples in addition to pure PMMA and pure PSF.

## 1.12 Thesis Layout

The thesis consists of five chapters of chapter one provides an introduction of the concepts and terminology as stated in the thesis with the problem statement and aims. Chapter two gives a literature review. Chapter 3 describes the materials and a sample preparation method, moreover includes a detailed explanation of the devices that used in the project. Chapter four illustrates the results of measurements have been reached and conclusions. Finally, Chapter 5 comprises the summary and future studies.



## REFERENCES

- Abdul Mannan, H., Mukhtar, H., Shima Shaharun, M., Roslee Othman, M., and Murugesan, T. (2016). Polysulfone/poly (ether sulfone) blended membranes for CO<sub>2</sub> separation. *Journal of Applied Polymer Science*, 133(5).
- Abouelezz, M., and Waters, P. F. (1978). Studies on the Photodegradation of Poly (methyl methacrylate). : National Bureau Of Standards Washington D.C. National Engineering Lab.
- Abouelezz, M., and Waters, P. (1978). Studies on the photodegradation of poly (methyl methacrylate): DTIC Document.
- Aguilar, J., Bautista-Quijano, J., and Avilés, F. (2010). Influence of carbon nanotube clustering on the electrical conductivity of polymer composite films. *Express Polym Lett*, 4(5): 292-299.
- Ahmed, M. A., and Ebrahim, M. I. (2014). Effect of Zirconium Oxide Nano-Fillers Addition on the Flexural Strength, Fracture Toughness, and Hardness of Heat-Polymerized Acrylic Resin. *World Journal of Nano Science and Engineering*, 2014.
- Ahmed, R. (2009). Optical study on poly (methyl methacrylate)/poly (vinyl acetate) blends. *International Journal of Photoenergy*, 2009.
- Ali, A., Yunus, R. M., Awang, M., and Yunus, M. A. C. (2015). Influence of Hydrophilic Polymer on Proteins Separation, Molecular Weight Cut-off (MWCO) and Average Pore Size of Polysulfone Blend Membrane. *Jurnal Teknologi*, 74(7).
- Aliabad, H. R., Bazrafshan, M., Vaezi, H., Yousaf, M., Munir, J., and Saeed, M. (2013). Optoelectronic Properties of Pure and Co Doped Indium Oxide by Hubbard and modified Becke–Johnson Exchange Potentials. *Chinese Physics Letters*, 30(12): 127101.
- Altinkok, C., Kiskan, B., and Yagci, Y. (2011). Synthesis and characterization of sulfone containing main chain oligobenzoxazine precursors. *Journal of Polymer Science Part A: Polymer Chemistry*, 49(11): 2445-2450.
- Asha, S., Demappa, T., Sanjeev, G., Parameswara, P., and Somashekar, R. (2009). Spectroscopic and thermal studies of 8MeV electron beam irradiated HPMC films. *Nuclear Instruments and Methods in Physics Research Section B: Beam Interactions with Materials and Atoms*, 267(14): 2385-2389.
- Ayeshamariam, A., Bououdina, M., and Sanjeeviraja, C. (2013). Optical, electrical and sensing properties of In<sub>2</sub>O<sub>3</sub> nanoparticles. *Materials Science in Semiconductor Processing*, 16(3): 686-695.
- Babizhayev, M. A., and Chumayevskii, N. A. (1994). Tinting effect of ultraviolet radiation on intraocular lenses of polymethyl methacrylate. *Bio-medical materials and engineering*, 4(1): 1-16.
- Bahrmann, H., Hahn, H., Mayer, D., and Frey, G. (2013). Ullmann's Encyclopedia of Industrial Chemistry: 2-Ethylhexanol: New York, NY: Wiley-VCH.

- Bath, P., Romberger, A., and Brown, P. (1986). A comparison of Nd: YAG laser damage thresholds for PMMA and silicone intraocular lenses. *Investigative ophthalmology and visual science*, 27(5): 795-798.
- Bautista-Quijano, J., Aviles, F., Aguilar, J., and Tapia, A. (2010). Strain sensing capabilities of a piezoresistive MWCNT-polysulfone film. *Sensors and Actuators A: Physical*, 159(2): 135-140.
- Bhat, D. K., and Jois, H. S. (2014). Miscibility and Conductivity Studies of Poly (methyl methacrylate) and Cellulose Acetate Phthalate Blends. *Procedia Materials Science*, 5: 995-1004.
- Bhat, D. K., and Kumar, M. S. (2006). Biodegradability of PMMA blends with some cellulose derivatives. *Journal of Polymers and the Environment*, 14(4): 385-392.
- Bourara, H., Hadjout, S., Benabdelghani, Z., and Etxeberria, A. (2014). Miscibility and Hydrogen Bonding in Blends of Poly (4-vinylphenol)/Poly (vinyl methyl ketone). *Polymers*, 6(11): 2752-2763.
- Bourdelais, R. P., and Greener, J. (2006). U.S. Patent No. 11,500,181.
- Bower, D. I. (2002). *An introduction to polymer physics*. New York: Cambridge University Press.
- Bronzino, J. D., and Peterson, D. R. (2014). *Biomedical engineering fundamentals*. Florida: CRC Press.
- Buruiana, L.-I., Avram, E., Popa, A., Musteata, V. E., and Ioan, S. (2012). Electrical conductivity and optical properties of a new quaternized polysulfone. *Polymer bulletin*, 68(6): 1641-1661.
- Busch, G., and Schade, H. (2013). *Lectures on Solid State Physics: International Series in Natural Philosophy* (Vol. 79). Hungary: Elsevier.
- Cai, X. G., Dai, M. H., Ji, X. L., Mei, Z. X., and Long, X. H. (2011). Preparation and ordered self-assembly of nano-Pd-Ga/PMMA by ultrasonic. *Journal of Nanomaterials*, 2011, 10.
- Cao, J., and Bhoyro, A. Y. (2001). Structural characterization of wool by thermal mechanical analysis of yarns. *Textile Research Journal*, 71(1): 63-66.
- Casas, J. S., and Sordo, J. (2011). *Lead: chemistry, analytical aspects, environmental impact and health effects*. Amsterdam: Elsevier.
- Celli, A., Marchese, P., Vannini, M., Berti, C., Fortunati, I., Signorini, R., and Bozio, R. (2011). Synthesis of novel fullerene-functionalized polysulfones for optical limiting applications. *Reactive and Functional Polymers*, 71(6): 641-647.
- Chandradass, J., Bae, D. S., and Kim, K. H. (2011). A simple method to prepare indium oxide nanoparticles: structural, microstructural and magnetic properties. *Advanced Powder Technology*, 22(3): 370-374.
- Chaturvedi, K., Kulkarni, A. R., and Aminabhavi, T. M. (2011). Blend microspheres of poly (3-hydroxybutyrate) and cellulose acetate phthalate for colon delivery

of 5-fluorouracil. *Industrial and Engineering Chemistry Research*, 50(18): 10414-10423.

- Cheerarat, O. (2012). The effects of nanoparticles on structure development in immiscible polymer blends. The University of Manchester. Manchester.
- Chen, L.-S., Huang, Z.-M., Dong, G.-H., He, C.-L., Liu, L., Hu, Y.-Y., and Li, Y. (2009). Development of a transparent PMMA composite reinforced with nanofibers. *Polymer Composites*, 30(3): 239.
- Cheng, S. Z. (2002). *Handbook of thermal analysis and calorimetry: applications to polymers and plastics* (Vol. 3). Amsterdam: Elsevier.
- Cowley, P., and Melville, H. (1952). *The Photo-Degradation of Polymethylmethacrylate. I. The Mechanism of Degradation*. Paper presented at the Proceedings of the Royal Society of London A: Mathematical, Physical and Engineering Sciences.
- Cowley, P., and Melville, H. (1952). *The Photo-Degradation of Polymethylmethacrylate. II. Evaluation of Absolute Rate Constants for a Depolymerization Reaction*. Paper presented at the Proceedings of the Royal Society of London A: Mathematical, Physical and Engineering Sciences.
- Delaby, I., Ernst, B., Froelich, D., and Muller, R. (1996). Droplet deformation in immiscible polymer blends during transient uniaxial elongational flow. *Polymer Engineering and Science*, 36(12): 1627-1635.
- Demir, M. M., Koynov, K., Akbey, U., Bubeck, C., Park, I., Lieberwirth, I., and Wegner, G. (2007). Optical properties of composites of PMMA and surface-modified zincite nanoparticles. *Macromolecules*, 40(4): 1089-1100.
- Diez-Pascual, A. M., Ashrafi, B., Naffakh, M., Gonzalez-Dominguez, J. M., Johnston, A., Simard, B., Gomez-Fatou, M. A. (2011). Influence of carbon nanotubes on the thermal, electrical and mechanical properties of poly (ether ether ketone)/glass fiber laminates. *Carbon*, 49(8): 2817-2833.
- Diez-Pascual, A. M., Naffakh, M., Gonzalez-Domínguez, J. M., Ansón, A., Martínez-Rubi, Y., Martínez, M. T., Gómez, M. A. (2010a). High performance PEEK/carbon nanotube composites compatibilized with polysulfones-I. Structure and thermal properties. *Carbon*, 48(12): 3485-3499.
- Diez-Pascual, A. M., Naffakh, M., Gonzalez-Domínguez, J. M., Ansón, A., Martínez-Rubi, Y., Martínez, M. T., Go mez, M. A. (2010b). High performance PEEK/carbon nanotube composites compatibilized with polysulfones-II. Mechanical and electrical properties. *Carbon*, 48(12): 3500-3511.
- Dinunzio, J. C., Miller, D. A., Yang, W., McGinity, J. W., and Williams III, R. O. (2008). Amorphous compositions using concentration enhancing polymers for improved bioavailability of itraconazole. *Molecular pharmaceuticals*, 5(6): 968-980.
- Dixit, M., Mathur, V., Gupta, S., Baboo, M., Sharma, K., and Saxena, N. (2009). Morphology, miscibility and mechanical properties of PMMA/PC blends. *Phase Transitions*, 82(12): 866-878.

- Dizman, C., Ates, S., Torun, L., and Yagci, Y. (2010). Synthesis, characterization and photoinduced curing of polysulfones with (meth) acrylate functionalities. *Beilstein journal of organic chemistry*, 6(1): 56.
- Dobos, A. M., Onofrei, M.-D., Tudorachi, N., and Ioan, S. (2015). Structural Orientations of Cellulose Acetate Phthalate/Ethyl Cellulose Blends in Solution. *Journal of Macromolecular Science, Part B*, 54(9): 1092-1104.
- Dobos, A. M., Onofrei, M. D., Stoica, I., Olaru, N., Olaru, L., and Ioan, S. (2012). Rheological properties and microstructures of cellulose acetate phthalate/hydroxypropyl cellulose blends. *Polymer Composites*, 33(11): 2072-2083.
- Dole, M. (2013). *The radiation chemistry of macromolecules* (Vol. 2). New York: Elsevier.
- Du, N., Zhang, H., Chen, B., Ma, X., Liu, Z., Wu, J., and Yang, D. (2007). Porous Indium Oxide Nanotubes: Layer - by - Layer Assembly on Carbon - Nanotube Templates and Application for Room - Temperature NH<sub>3</sub> Gas Sensors. *Advanced Materials*, 19(12): 1641-1645.
- Duan, P., Agrawal, G., and Walls, C. (2011). U.S. Patent No. 13,118,998.
- Duval-Terrié, C., and Lebrun, L. (2006). Polymerization and Characterization of PMMA. Polymer Chemistry Laboratory Experiments for Undergraduate Students. *Journal of chemical education*, 83: 443.
- Ebewele, R. O. (2000). *Polymer science and technology*. Florida: CRC press.
- Edgar, K. J., Buchanan, C. M., Debenham, J. S., Rundquist, P. A., Seiler, B. D., Shelton, M. C., and Tindall, D. (2001). Advances in cellulose ester performance and application. *Progress in polymer science*, 26(9): 1605-1688.
- Edwards, D. L., Finckenor, M. M., O'Neill, M. J., and McDanal, A. (2000). *Optical analysis of transparent polymeric material exposed to simulated space environment*. Paper presented at the International Symposium on Optical Science and Technology.
- El-Hibri, M. J. (2008). U.S. Patent No. 7,423,110.
- El-Zaher, N. A., Melegy, M. S., and Guirguis, O. W. (2014). Thermal and Structural Analyses of PMMA/TiO<sub>2</sub> Nanoparticles Composites. *Natural Science*, 6(11): 859-870.
- El - Hibri, M. J., and Weinberg, S. A. (2001). Polysulfones. *Encyclopedia of Polymer Science and Technology*. New York: John Wiley and Sons, Inc.
- El Haitami, A., Backus, E. H., and Cantin, S. (2014). Synthesis at the Air–Water Interface of a Two-Dimensional Semi-Interpenetrating Network Based on Poly (dimethylsiloxane) and Cellulose Acetate Butyrate. *Langmuir*, 30(40): 11919-11927.
- Elemans, P., Janssen, J., and Meijer, H. (1990). The measurement of interfacial tension in polymer/polymer systems: The breaking thread method. *Journal of Rheology (1978-present)*, 34(8): 1311-1325.

- Eustis, S., and El-Sayed, M. A. (2006). Why gold nanoparticles are more precious than pretty gold: noble metal surface plasmon resonance and its enhancement of the radiative and nonradiative properties of nanocrystals of different shapes. *Chemical society reviews*, 35(3): 209-217.
- Faria, R., Duncan, J. C., and Brereton, R. G. (2007). Dynamic mechanical analysis and chemometrics for polymer identification. *Polymer testing*, 26(3): 402-412.
- Fekete, E., and Pukanszky, B. (2005). Effect of molecular interactions on the miscibility and structure of polymer blends. *European Polymer Journal*, 41(4): 727-736.
- Fink, D. (2004). *Fundamentals of ion-irradiated polymers* (Vol. 63). New York: Springer Science and Business Media.
- Fraih, M. (2010). *Study of Thermal Aging Effect on Optical Properties of Some Polymer Blends*. University of Technology, Baghdad.
- Freeman, A., Mantell, S. C., and Davidson, J. H. (2005). Mechanical performance of polysulfone, polybutylene, and polyamide 6/6 in hot chlorinated water. *Solar energy*, 79(6): 624-637.
- Fried, J. R. (2014). *Polymer science and technology*. New Jersey: Pearson Education.
- Gabbott, P. (2008). *Principles and applications of thermal analysis*. New Delhi: John Wiley and Sons.
- Gadag, R., and Shetty, A. N. (2007). *Engineering Chemistry*. New Delhi: IK International Pvt Ltd.
- Ganeev, R., Rysanyanskiy, A., Chakravarty, U., Naik, P., Srivastava, H., Tiwari, M., and Gupta, P. (2007). Structural, optical, and nonlinear optical properties of indium nanoparticles prepared by laser ablation. *Applied Physics B*, 86(2): 337-341.
- Gaur, M., Singh, P. K., and Chauhan, R. (2013). Structural and thermal properties of polysulfone-ZnO nanocomposites. *Journal of thermal analysis and calorimetry*, 111(1): 743-751.
- Gaurav, A., Ashamol, A., Deepthi, M., and Sailaja, R. (2012). Biodegradable nanocomposites of cellulose acetate phthalate and chitosan reinforced with functionalized nanoclay: Mechanical, thermal, and biodegradability studies. *Journal of Applied Polymer Science*, 125(S1).
- Gleiter, H. (2000). Nanostructured materials: basic concepts and microstructure. *Acta materialia*, 48(1): 1-29.
- Goldstein, J. (2012). *Practical scanning electron microscopy: electron and ion microprobe analysis*. New York: Springer Science and Business Media.
- Gomes, G. d. S., Almeida, A. T. d., Kosaka, P. M., Rogero, S. O., Cruz, Á. S., Ikeda, T. I., and Petri, D. F. S. (2007). Cellulose acetate propionate coated titanium:

- characterization and biotechnological application. *Materials Research*, 10(4): 469-474.
- Grattan, K. T., and Meggitt, B. T. (1995). *Optical fiber sensor technology* (Vol. 1). London: Chapman and Hall.
- Guinier, A. (1994). *X-ray diffraction in crystals, imperfect crystals, and amorphous bodies*. New York: Courier Corporation.
- Guo, H., Packirisamy, S., Mani, R., Aronson, C., Gvozdic, N., and Meier, D. (1998). Compatibilizing effects of block copolymers in low-density polyethylene/polystyrene blends. *Polymer*, 39(12): 2495-2505.
- Gupta, P., and Singh, K. (1996). Characterization of H 3 PO 4 based PVA complex system. *Solid State Ionics*, 86: 319-323.
- Hamdy, M. S., AlFaify, S., Al-Hajry, A., and Yahia, I. S. (2016). Optical constants, photo-stability and photo-degradation of MB/PMMA thin films for UV sensors. *Optik-International Journal for Light and Electron Optics*, 127(12): 4959-4963.
- Hanafi, A., Nograles, N., Abdullah, S., Shamsudin, M. N., and Rosli, R. (2013). Cellulose acetate phthalate microencapsulation and delivery of plasmid DNA to the intestines. *Journal of pharmaceutical sciences*, 102(2): 617-626.
- Harper, C. A. (2006). *Handbook of plastic processes*. New Jersey: John Wiley and Sons.
- He, Y., Zhu, B., and Inoue, Y. (2004). Hydrogen bonds in polymer blends. *Progress in polymer science*, 29(10): 1021-1051.
- Heijboer, J., Baas, J., Van d. G., B., and Hoefnagel, M. (1987). A molecular mechanics study on rotational motions of side groups in poly (methyl methacrylate). *Polymer*, 28(3): 509-513.
- Hoek, E. M., Peng, F., and Jinwen, W. A. N. G. (2011). U.S. Patent No. 13,697,277.
- Holland, B., and Hay, J. (2001). The kinetics and mechanisms of the thermal degradation of poly (methyl methacrylate) studied by thermal analysis-Fourier transform infrared spectroscopy. *Polymer*, 42(11): 4825-4835.
- Huang, F. Y. (2012). Thermal properties and thermal degradation of cellulose tri-stearate (CTs). *Polymers*, 4(2): 1012-1024.
- Hugi, R., and Geva, H. (2005). U.S. Patent No. 11,209,726.
- Ibrahim, B. A., and Kadum, K. M. (2010). Influence of polymer blending on mechanical and thermal properties. *Modern Applied Science*, 4(9): 157.
- Iwamoto, S., Nakagaito, A., Yano, H., and Nogi, M. (2005). Optically transparent composites reinforced with plant fiber-based nanofibers. *Applied Physics A*, 81(6): 1109-1112.
- Jeong, H., Rooney, M., David, D., MacKnight, W., Karasz, F., and Kajiyama, T. (2000). Miscibility and characterization of the ternary crystalline system:

poly (vinyl butyral)/poly (vinyl alcohol)/nylon6. *Polymer*, 41(17): 6671-6678.

Kaczmarek, H., and Galka, P. (2008). Effect of Irgacure 651 Initiator on Poly (Methyl Methacrylate) Photostability Studied by UV-Vis Spectroscopy. *The Open Process Chemistry Journal*, 1(1).

Kandare, E., Deng, H., Wang, D., and Hossenlopp, J. M. (2006). Thermal stability and degradation kinetics of poly (methyl methacrylate)/layered copper hydroxy methacrylate composites. *Polymers for advanced technologies*, 17(4): 312-319.

Kanis, L. A., Marques, E. L., Zepon, K. M., Pereira, J. R., Pamato, S., de Oliveira, M. T., Petronilho, F. C. (2014). Cellulose acetate butyrate/poly (caprolactonetriol) blends: Miscibility, mechanical properties, and in vivo inflammatory response. *Journal of biomaterials applications*, 29(5): 654-661.

Karak, N. (2009). *Fundamentals of polymers: raw materials to finish products*. New Delhi: PHI Learning Pvt. Ltd.

Karazhanov, S. Z., Ravindran, P., Vajeeston, P., Ulyashin, A., Finstad, T., and Fjellvåg, H. (2007). Phase stability, electronic structure, and optical properties of indium oxide polytypes. *Physical Review B*, 76(7): 075129.

Kashiwagi, T., Inaba, A., Brown, J. E., Hatada, K., Kitayama, T., and Masuda, E. (1986). Effects of weak linkages on the thermal and oxidative degradation of poly (methyl methacrylates). *Macromolecules*, 19(8): 2160-2168.

Kim, H. S., Byrne, P. D., Facchetti, A., and Marks, T. J. (2008). High performance solution-processed indium oxide thin-film transistors. *Journal of the American Chemical Society*, 130(38): 12580-12581.

Kine, B., and Novak, R. (1985). Acrylic and methacrylic ester polymers. *Wiley-Interscience, Encyclopedia of Polymer Science and Engineering*, 1: 234-286.

Kogej, K., Orel, Z. C., and Žigon, M. (2011). Polyol mediated nano size zinc oxide and nanocomposites with poly (methyl methacrylate). *Express Polymer Letters*, 5(7).

Kos, T., Anžlovar, A., Pahovnik, D., Žagar, E., Orel, Z. C., and Žigon, M. (2013). Zinc-containing block copolymer as a precursor for the in situ formation of nano ZnO and PMMA/ZnO nanocomposites. *Macromolecules*, 46(17): 6942-6948.

Kotsilkova, R., Fragiadakis, D., and Pissis, P. (2005). Reinforcement effect of carbon nanofillers in an epoxy resin system: rheology, molecular dynamics, and mechanical studies. *Journal of Polymer Science Part B: Polymer Physics*, 43(5): 522-533.

Krishnaswamy, R. K., Wadud, S. E. B., and Baird, D. G. (1999). Influence of a reactive terpolymer on the properties of in situ composites based on polyamides and thermotropic liquid crystalline polyesters. *Polymer*, 40(3): 701-716.

- Kumar, V., and Singh, J. (2010). Model for calculating the refractive index of different materials. *Indian journal of pure and applied physics*, 48(8): 571-574.
- Kutz, M. (2011). *Applied plastics engineering handbook: processing and materials*. Oxford: William Andrew.
- Kwei, T., Pearce, E. M., Pennacchia, J. R., and Charton, M. (1987). Correlation between the glass transition temperatures of polymer mixtures and intermolecular force parameters. *Macromolecules*, 20(5): 1174-1176.
- Kuzyk, M. G. (2006). *Polymer Fiber Optics: materials, physics, and applications*, Florida: CRC press.
- Lavoine, N., Desloges, I., Dufresne, A., and Bras, J. (2012). Microfibrillated cellulose—Its barrier properties and applications in cellulosic materials: A review. *Carbohydrate polymers*, 90(2): 735-764.
- Lee, E. S., Hong, S. K., Kim, Y. S., Lee, J. H., and Won, J. C. (2008). Preparation and characteristics of cross - linkable polysulfone having methylene methacrylate side - chain. *Journal of Applied Polymer Science*, 109(1): 1-8.
- Lee, K. J., Jho, J. Y., Kang, Y. S., Won, J., Dai, Y., Robertson, G. P., and Guiver, M. D. (2003). Gas transport and dynamic mechanical behavior in modified polysulfones with trimethylsilyl groups: effect of degree of substitution. *Journal of membrane science*, 223(1): 1-10.
- Liu, C., Luo, Y., Jia, Z., Zhong, B., Li, S., Guo, B., and Jia, D. (2011). Enhancement of mechanical properties of poly (vinyl chloride) with polymethyl methacrylate-grafted halloysite nanotube. *Express Polym Lett*, 5(7): 591-603.
- Liu, H., Liu, D., Yao, F., and Wu, Q. (2010). Fabrication and properties of transparent polymethylmethacrylate/cellulose nanocrystals composites. *Bioresource Technology*, 101(14): 5685-5692.
- Liu, L., Tong, C., He, Y., Zhao, Y., Hu, B., and Lü, C. (2015). Novel quaternized mesoporous silica nanoparticle modified polysulfone-based composite anion exchange membranes for alkaline fuel cells. *RSC Advances*, 5(54): 43381-43390.
- Lokensgard, E. (2016). *Industrial plastics: theory and applications*. New York: Nelson Education.
- Lu, X., and Weiss, R. (1992). Relationship between the glass transition temperature and the interaction parameter of miscible binary polymer blends. *Macromolecules*, 25(12): 3242-3246.
- Maensiri, S., Laokul, P., Klinkaewnarong, J., Phokha, S., Promarak, V., and Seraphin, S. (2008a). Indium oxide (In<sub>2</sub>O<sub>3</sub>) nanoparticles using Aloe vera plant extract: Synthesis and optical properties. *J Optoelectron Adv Mater*, 10: 161-165.
- Maensiri, S., Laokul, P., Klinkaewnarong, J., Phokha, S., Promarak, V., and Seraphin, S. (2008b). Indium oxide (In<sub>2</sub>O<sub>3</sub>) nanoparticles using Aloe vera

- plant extract: Synthesis and optical properties. *J Optoelectron Adv Mater*, 10: 161-165.
- Malek, C. K., and Duffait, R. (2007). Packaging using hot-embossing with a polymeric intermediate mould. *The International Journal of Advanced Manufacturing Technology*, 33(1-2): 187-190.
- Manaf, M. E. A., Tsuji, M., Nobukawa, S., and Yamaguchi, M. (2011). Effect of moisture on the orientation birefringence of cellulose esters. *Polymers*, 3(2): 955-966.
- Manring, L. E., Sogah, D. Y., and Cohen, G. M. (1989). Thermal degradation of poly (methyl methacrylate). 3. Polymer with head-to-head linkages. *Macromolecules*, 22(12): 4652-4654.
- Margolis, J. (1985). Engineering thermoplastics: properties and applications. *Plast. Eng.*, 41(11): 63.
- Margolis, J. (2012). *Conductive polymers and plastics*. New York: Springer Science and Business Media.
- Marin, L., and Perju, E. (2009). Polysulfone as polymer matrix for a novel polymer-dispersed liquid crystals system. *Phase Transitions*, 82(7): 507-518.
- Mark, H. F. (2013). *Encyclopedia of polymer science and technology, concise*. New Jersey: John Wiley and Sons.
- Menard, K. P. (2008). *Dynamic mechanical analysis: a practical introduction*. New York: CRC press.
- Merenga, A. S., and Katana, G. (2010). Dynamic mechanical analysis of PMMA-cellulose blends. *International Journal of Polymeric Materials*, 60(2): 115-123.
- Michelson, J., Werner, L., Ollerton, A., Leishman, L., and Bodnar, Z. (2012). Light scattering and light transmittance in intraocular lenses explanted because of optic opacification. *Journal of Cataract and Refractive Surgery*, 38(8): 1476-1485.
- Miracle, D. B., and Donaldson, S. L. (2003). Air force research laboratory. *Introduction to Composites, ASM International, Composites, 21*.
- Mitsuoka, T., Torikai, A., and Fueki, K. (1993). Wavelength sensitivity of the photodegradation of poly (methyl methacrylate). *Journal of Applied Polymer Science*, 47(6): 1027-1032.
- Mohanty, A., Drzal, L., Park, H., Misra, M., and Wibowo, A. (2005). U.S. Patent No. 11,111,362.
- Momeni, S., and Pakizeh, M. (2013). Preparation, characterization and gas permeation study of PSf/MgO nanocomposite membrane. *Brazilian Journal of Chemical Engineering*, 30(3): 589-597.
- Murali, A., Barve, A., Leppert, V. J., Risbud, S. H., Kennedy, I. M., and Lee, H. W. (2001). Synthesis and characterization of indium oxide nanoparticles. *Nano Letters*, 1(6): 287-289.

- Nayak, L., Rahaman, M., Khastgir, D., and Chaki, T. (2011). Thermal and electrical properties of carbon nanotubes based polysulfone nanocomposites. *Polymer bulletin*, 67(6): 1029-1044.
- Neurath, A. R. (2002). U.S. Patent No. 6,462,030.
- Nicholson, J. W. (2012). *The chemistry of polymers*: Royal Society of Chemistry.
- Nobukawa, S., Aoki, Y., Yoshimura, H., Tachikawa, Y., and Yamaguchi, M. (2013). Effect of aromatic additives with various alkyl groups on orientation birefringence of cellulose acetate propionate. *Journal of Applied Polymer Science*, 130(5): 3465-3472.
- Nobukawa, S., Hayashi, H., Shimada, H., Kiyama, A., Yoshimura, H., Tachikawa, Y., and Yamaguchi, M. (2014). Strong orientation correlation and optical anisotropy in blend of cellulose ester and poly (ethylene 2, 6 - naphthalate) oligomer. *Journal of Applied Polymer Science*, 131(15).
- Nogi, M., Ifuku, S., Abe, K., Handa, K., Nakagaito, A. N., and Yano, H. (2006). Fiber-content dependency of the optical transparency and thermal expansion of bacterial nanofiber reinforced composites. *Applied Physics Letters*, 88(13).
- Obie, R. (2006). U.S. Patent No. 7,026,470.
- Ohno, T., and Nishio, Y. (2007). Molecular orientation and optical anisotropy in drawn films of miscible blends composed of cellulose acetate and poly (N-vinylpyrrolidone-co-methyl methacrylate). *Macromolecules*, 40(9): 3468-3476.
- Olabisi, O., and Adewale, K. (1997). *Handbook of thermoplastics* (Vol. 41). Florida: CRC press.
- Olmos, D., Prolongo, S., and González-Benito, J. (2014). Thermo-mechanical properties of polysulfone based nanocomposites with well dispersed silica nanoparticles. *Composites Part B: Engineering*, 61: 307-314.
- Orlandi, M. O., Aguiar, R., Lanfredi, A., Longo, E., Varela, J. A., and Leite, E. (2005). Tin-doped indium oxide nanobelts grown by carbothermal reduction method. *Applied Physics A*, 80(1): 23-25.
- Osuagwu, U. L., and Ogbuehi, K. C. (2014). UV-vis light transmittance through tinted contact lenses and the effect of color on values. *Contact Lens and Anterior Eye*, 37(3): 136-143.
- Otsuka, T., and Chujo, Y. (2010). Poly (methyl methacrylate)(PMMA)-based hybrid materials with reactive zirconium oxide nanocrystals. *Polymer journal*, 42(1): 58-65.
- Otto, R., and Walter, B. (1940). Glass substitute and process of preparing: US Patent No. 2,193,742.
- Park, J. W., Tanaka, T., and Iwata, T. (2005). Uniaxial Drawing of Poly [(R) - 3 - hydroxybutyrate]/Cellulose Acetate Butyrate Blends and Their Orientation Behavior. *Macromolecular bioscience*, 5(9): 840-852.

- Patricia Allue, D., and Vagner Roberto, B. (2012). Synthesis and Characterization of a New Cellulose Acetate-Propionate Gel: Crosslinking Density Determination. *Open Journal of Polymer Chemistry*, 2012.
- Paul, D. R. (2012). *Polymer blends* (Vol. 1). New York: Elsevier.
- Peng, G., Li, Q., Yang, Y., and Wang, H. (2009). Degradation of nano ZnO - glass fiber - unsaturated polyester composites. *Journal of Applied Polymer Science*, 114(4): 2128-2133.
- Perju, E., Marin, L., Grigoras, V. C., and Bruma, M. (2011). Thermotropic and optical behaviour of new PDLC systems based on a polysulfone matrix and a cyanoazomethine liquid crystal. *Liquid Crystals*, 38(7): 893-905.
- Pokropivny, V. (2007). *Introduction to nanomaterials and nanotechnology*. Tartu: Tartu University Press.
- Poomalai, P., and Varghese, T. (2011). Thermomechanical Behaviour of Poly (methyl methacrylate)/Copoly (ether-ester) Blends. *ISRN Materials Science*, 2011.
- Prasad, P. N. (2012). *Frontiers of polymers and advanced materials*. New York: Springer Science and Business Media.
- Rabek, J. F., and Fouassier, J.-P. (1989). *Lasers in polymer science and technology: applications* (Vol. 1). Florida: CRC Press.
- Rafiq, S., Man, Z., Maitra, S., Muhammad, N., and Ahmad, F. (2012). Kinetics of thermal degradation of polysulfone/polyimide blended polymeric membranes. *Journal of Applied Polymer Science*, 123(6): 3755-3763.
- Reddy, R., Ahammed, Y. N., Gopal, K. R., and Raghuram, D. (1998). Optical electronegativity and refractive index of materials. *Optical materials*, 10(2): 95-100.
- Reyes A., M. A., Torres-Huerta, A. M., Domínguez-Crespo, M. A., Flores-Vela, A. I., Dorantes-Rosales, H. J., and Andraca-Adame, J. A. (2015). Thermal, mechanical and UV-shielding properties of poly (methyl methacrylate)/cerium dioxide hybrid systems obtained by melt compounding. *Polymers*, 7(9): 1638-1659.
- Rich, R. (2005). Cellulose Ester Plastics (Organic). *Van Nostrand's Encyclopedia of Chemistry*. New York: John Wiley and Sons, Inc.
- Rieger, J. (2001). The glass transition temperature  $T_g$  of polymers—comparison of the values from differential thermal analysis (DTA, DSC) and dynamic mechanical measurements (torsion pendulum). *Polymer testing*, 20(2): 199-204.
- Robeson, L. (2014). Historical Perspective of Advances in the Science and Technology of Polymer Blends. *Polymers*, 6(5): 1251-1265.
- Rowen, J. W., Hunt, C. M., and Plyler, E. K. (1947). Absorption spectra in the detection of chemical changes in cellulose and cellulose derivatives. *Textile Research Journal*, 17(9): 504-511.

- Rupiasih, N. N., Suyanto, H., Sumadiyasa, M., and Wendri, N. (2013). Study of effects of low doses UV radiation on microporous polysulfone membranes in sterilization process. *Open Journal of Organic Polymer Materials*, 3(1): 12-18.
- Russo, J. M., and Shea, T. M. (2013). U.S. Patent No. 13,926,634.
- Rusu, G., Airinei, A., Hamciuc, V., Rusu, G., Râmbu, P., Diciu, M., Rusu, M. (2009). Electronic and optical properties of some polysulfone-polydimethylsiloxane copolymers in thin films. *Journal of Macromolecular Science*, 48(2): 238-253.
- Ryan, A. J. (1998). *Polymer processing and structure development*. Dordrecht: Springer Science and Business Media.
- Said, K. A., Amiin, I. S., Zhang, H., and Pan, M. (2014). Functionalized Polysulfones as an Alternative Material to Improve Proton Conductivity at Low Relative Humidity Fuel Cell Applications. *Chemistry and Materials Research*, 6(2): 19-29.
- Sailaja, R., and Seetharamu, S. (2009). Mechanical and thermal properties of LDPE - cellulose acetate phthalate blends—Effect of maleic anhydride - grafted LDPE compatibilizer. *Journal of Applied Polymer Science*, 112(2): 649-659.
- Schneider, M., Meier, P., and Kornmann, X. (2012). U.S. Patent No. 13/685,142.
- Scott, C. E., and Macosko, C. W. (1995). Morphology development during the initial stages of polymer-polymer blending. *Polymer*, 36(3): 461-470.
- Selvakumar, M., and Krishna Bhat, D. (2008). Miscibility of poly (methylmethacrylate) and cellulose acetate butyrate blends in dimethyl formamide. *Indian Journal of Chemical Technology*, 15(6): 547.
- Seymour, R. B., and Carraher, C. E. (1984). *Structure-property relationships in polymers*. New York: Plenum Press.
- Shanbhag, A., Barclay, B., Koziara, J., and Shivanand, P. (2007). Application of cellulose acetate butyrate-based membrane for osmotic drug delivery. *Cellulose*, 14(1): 65-71.
- Shih, J. S., and Musa, O. M. (2014). U.S. Patent No. 8,673,272.
- Shih, Y. C., Qiu, C. X., Shih, I., and Qiu, C. (2007). U.S. Patent No. 7,211,825.
- Shimazaki, Y., Miyazaki, Y., Takezawa, Y., Nogi, M., Abe, K., Ifuku, S., and Yano, H. (2007). Excellent thermal conductivity of transparent cellulose nanofiber/epoxy resin nanocomposites. *Biomacromolecules*, 8(9): 2976-2978.
- Silverstein, R. M., Webster, F. X., Kiemle, D., and Bryce, D. L. (2014). *Spectrometric identification of organic compounds*. New York: John Wiley and Sons.

- Singhal, A., Dubey, K., Bhardwaj, Y., Jain, D., Choudhury, S., and Tyagi, A. (2013). UV-shielding transparent PMMA/In<sub>2</sub>O<sub>3</sub> nanocomposite films based on In<sub>2</sub>O<sub>3</sub> nanoparticles. *RSC Advances*, 3(43): 20913-20921.
- Sood, V. (2007). *An Experimental Study on Thermal Bonding Effects of PMMA based Micro-devices using Hot Embossing*: University of Texas, Texas.
- Soumya, S., Mohamed, A. P., Paul, L., Mohan, K., and Ananthakumar, S. (2014). Near IR reflectance characteristics of PMMA/ZnO nanocomposites for solar thermal control interface films. *Solar Energy Materials and Solar Cells*, 125: 102-112.
- Souza, D., Castillo, T. E., and Rodríguez, R. J. S. (2012). Effects of hydroxyvalerate contents in thermal degradation kinetic of cellulose acetate propionate/poly (3-hydroxyalkanoates) blends. *Journal of thermal analysis and calorimetry*, 109(3): 1353-1364.
- Souza, E., Rey, J., and Muccillo, E. (2009). Synthesis and characterization of spherical and narrow size distribution indium oxide nanoparticles. *Applied surface science*, 255(6): 3779-3783.
- Strong, A. B. (2006). *Plastics: materials and processing*: Prentice Hall.
- SU'AD, D. A., and ISMAIL, I. M. (2008). PMMA degradation protection investigation using ultraviolet additive. *Oriental Journal of Chemistry*, 24(1): 35-42.
- Subrahmanyam, S. (2003). *An Investigation of Pore Collapse in Asymmetric Polysulfone Membranes*. Virginia Polytechnic Institute and State University. Virginia.
- Sugumar, S., and Bellan, C. (2014). Transparent nano composite PVA–TiO<sub>2</sub> and PMMA–TiO<sub>2</sub> thin films: Optical and dielectric properties. *Optik-International Journal for Light and Electron Optics*, 125(18): 5128-5133.
- Sun, L., Gibson, R. F., Gordaninejad, F., and Suhr, J. (2009). Energy absorption capability of nanocomposites: a review. *Composites science and technology*, 69(14): 2392-2409.
- Sun, Y.-S., Wang, C.-T., and Liou, J.-Y. (2016). Tuning polymer-surface chemistries and interfacial interactions with UV irradiated polystyrene chains to control domain orientations in thin films of PS-b-PMMA. *Soft matter*, 12(11): 2923-2931.
- Suttiwijitpukdee, N., Sato, H., Zhang, J., and Hashimoto, T. (2011). Effects of intermolecular hydrogen bondings on isothermal crystallization behavior of polymer blends of cellulose acetate butyrate and poly (3-hydroxybutyrate). *Macromolecules*, 44(9): 3467-3477.
- Suttiwijitpukdee, N., Sato, H., Zhang, J., Hashimoto, T., and Ozaki, Y. (2011). Intermolecular interactions and crystallization behaviors of biodegradable polymer blends between poly (3-hydroxybutyrate) and cellulose acetate butyrate studied by DSC, FT-IR, and WAXD. *Polymer*, 52(2): 461-471.

- Tachibana, Y., Giang, N. T. T., Ninomiya, F., Funabashi, M., and Kunioka, M. (2010). Cellulose acetate butyrate as multifunctional additive for poly (butylene succinate) by melt blending: Mechanical properties, biomass carbon ratio, and control of biodegradability. *Polymer Degradation and Stability*, 95(8): 1406-1413.
- Takai, C., Fuji, M., and Takahashi, M. (2007). A novel surface designed technique to disperse silica nano particle into polymer. *Colloids and Surfaces A: Physicochemical and Engineering Aspects*, 292(1): 79-82.
- Tang, E., Cheng, G., and Ma, X. (2006). Preparation of nano-ZnO/PMMA composite particles via grafting of the copolymer onto the surface of zinc oxide nanoparticles. *Powder Technology*, 161(3): 209-214.
- Tang, Y. H., Lin, Y.-K., Zhou, B., and Wang, X.-L. (2016). PVDF membranes prepared via thermally induced (liquid–liquid) phase separation and their application in municipal sewage and industry wastewater for water recycling. *Desalination and Water Treatment*. 1-19.
- Tatsushima, T., Ogata, N., Nakane, K., and Ogihara, T. (2005). Structure and physical properties of cellulose acetate butyrate/poly (butylene succinate) blend. *Journal of Applied Polymer Science*, 96(2): 400-406.
- Torikai, A., and Hasegawa, H. (1998). Wavelength effect on the accelerated photodegradation of polymethylmethacrylate. *Polymer Degradation and Stability*, 61(2): 361-364.
- Torikai, A., Ohno, M., and Fueki, K. (1990). Photodegradation of poly (methyl methacrylate) by monochromatic light: Quantum yield, effect of wavelengths, and light intensity. *Journal of Applied Polymer Science*, 41(5 - 6): 1023-1032.
- Ursan, M., and Ursan, G.-A. (2011). Dielectric properties characterisation and 3D visualization and of nano-conductive. 4.
- Valles, C., Kinloch, I. A., Young, R. J., Wilson, N. R., and Rourke, J. P. (2013). Graphene oxide and base-washed graphene oxide as reinforcements in PMMA nanocomposites. *Composites science and technology*, 88: 158-164.
- Van Hest, M., Dabney, M., Perkins, J., Ginley, D., and Taylor, M. (2005). Titanium-doped indium oxide: A high-mobility transparent conductor. *Applied Physics Letters*, 87(3).
- Vinodh, R., Purushothaman, M., and Sangeetha, D. (2011). Novel quaternized polysulfone/ZrO<sub>2</sub> composite membranes for solid alkaline fuel cell applications. *international journal of hydrogen energy*, 36(12): 7291-7302.
- Vroman, I., and Tighzert, L. (2009). Biodegradable polymers. *Materials*, 2(2): 307-344.
- Wang, B., Tang, Q., Hong, N., Song, L., Wang, L., Shi, Y., and Hu, Y. (2011). Effect of cellulose acetate butyrate microencapsulated ammonium polyphosphate on the flame retardancy, mechanical, electrical, and thermal properties of intumescent flame-retardant ethylene–vinyl acetate

- copolymer/microencapsulated ammonium polyphosphate/polyamide-6 blends. *ACS applied materials and interfaces*, 3(9): 3754-3761.
- Wang, F., Tseng, S. C., Wang, X., Feng, K. C., Gu, H., Zang, H., and Liang, R. C. (2011). U.S. Patent No. 7,910,205.
- Wang, H., Xu, P., Zhong, W., Shen, L., and Du, Q. (2005). Transparent poly (methyl methacrylate)/silica/zirconia nanocomposites with excellent thermal stabilities. *Polymer Degradation and Stability*, 87(2): 319-327.
- Wang, K. (2008). Transparent oxide semiconductors: fabrication, properties, and applications. University of Waterloo. Ontario.
- Wojciechowska, P., and Foltynowicz, Z. (2009). Synthesis of organic-inorganic hybrids based on cellulose acetate butyrate. *Polimery*, 54(11-12): 845-848.
- Wu, P. S., Huang, L.-N., Guo, Y.-C., and Lin, C.-C. (2014). Effects of the novel poly (methyl methacrylate)(PMMA)-encapsulated organic ultraviolet (UV) filters on the UV absorbance and in vitro sun protection factor (SPF). *Journal of Photochemistry and Photobiology B: Biology*, 131: 24-30.
- Xing, C., Wang, H., Hu, Q., Xu, F., Cao, X., You, J., and Li, Y. (2013). Mechanical and thermal properties of eco-friendly poly (propylene carbonate)/cellulose acetate butyrate blends. *Carbohydrate polymers*, 92(2): 1921-1927.
- Xiong, H. M., Zhao, X., and Chen, J. S. (2001). New polymer-inorganic nanocomposites: PEO-ZnO and PEO-ZnO-LiClO<sub>4</sub> films. *The Journal of Physical Chemistry B*, 105(42): 10169-10174.
- Xiong, M., Gu, G., You, B., and Wu, L. (2003). Preparation and characterization of poly (styrene butylacrylate) latex/nano - ZnO nanocomposites. *Journal of Applied Polymer Science*, 90(7): 1923-1931.
- Yamaguchi, M., and Arakawa, K. (2007). Control of structure and mechanical properties for binary blends of poly (3 - hydroxybutyrate) and cellulose derivative. *Journal of Applied Polymer Science*, 103(5): 3447-3452.
- Yamaguchi, M., and Masuzawa, K. (2007). Birefringence control for binary blends of cellulose acetate propionate and poly (vinyl acetate). *European Polymer Journal*, 43(8): 3277-3282.
- Yamaguchi, M., and Masuzawa, K. (2008). Transparent polymer blends composed of cellulose acetate propionate and poly (epichlorohydrin). *Cellulose*, 15(1): 17-22.
- Yamaguchi, M., Okada, K., Manaf, M. E. A., Shiroyama, Y., Iwasaki, T., and Okamoto, K. (2009). Extraordinary wavelength dispersion of orientation birefringence for cellulose esters. *Macromolecules*, 42(22): 9034-9040.
- Yang, H., Ren, Q., Zhang, G., Chow, Y. T., Chan, H. P., and Chu, P. L. (2005). Preparation and optical constants of the nano-crystal and polymer composite Bi<sub>4</sub>Ti<sub>3</sub>O<sub>12</sub>/PMMA thin films. *Optics and Laser Technology*, 37(4): 259-264.

- Yano, H., Sugiyama, J., Nakagaito, A. N., Nogi, M., Matsuura, T., Hikita, M., and Handa, K. (2005). Optically transparent composites reinforced with networks of bacterial nanofibers. *Advanced Materials*, 17(2): 153-155.
- Yousif, E., El-Hiti, G. A., Haddad, R., and Balakit, A. A. (2015). Photochemical stability and photostabilizing efficiency of poly (methyl methacrylate) based on 2-(6-methoxynaphthalen-2-yl) propanoate metal ion complexes. *Polymers*, 7(6): 1005-1019.
- Yu, L. (2009). *Biodegradable polymer blends and composites from renewable resources*. New Jersey: John Wiley and Sons.
- Zang, H., Wang, F., Gu, H., and Liang, R. C. (2005). U.S. Patent Application No. 11,051,444.
- Zeng, H., Cai, W., Liu, P., Xu, X., Zhou, H., Klingshirn, C., and Kalt, H. (2008). ZnO-based hollow nanoparticles by selective etching: elimination and reconstruction of metal– semiconductor interface, improvement of blue emission and photocatalysis. *ACS nano*, 2(8): 1661-1670.
- Zhang, H., Zhang, P., Li, Z., Sun, M., Wu, Y., and Wu, H. (2007). A novel sandwiched membrane as polymer electrolyte for lithium ion battery. *Electrochemistry communications*, 9(7): 1700-1703.
- Zhang, J., and He, J. (2002). Interfacial compatibilization for PSF/TLCP blends by a modified polysulfone. *Polymer*, 43(4): 1437-1446.
- Zhang, J., and Liu, H. (2009). *Electrocatalysis of direct methanol fuel cells: from fundamentals to applications*. Darmstadt: John Wiley and Sons.
- Zhang, Y. (2008). *Geochemical kinetics*. Oxford: Princeton University Press.
- Zhou, C., Li, J., Chen, S., Wu, J., Heier, K. R., and Cheng, H. (2008). First-principles study on water and oxygen adsorption on surfaces of indium oxide and indium tin oxide nanoparticles. *The Journal of Physical Chemistry C*, 112(36): 14015-14020.
- Zhu, F. L., Feng, Q.-Q., Xin, Q., and Zhou, Y. (2014). Thermal degradation process of polysulfone aramid fiber. *Thermal Science*, 18(5): 1637-1641.
- Zweben, C. (1998). *Composite Materials and Mechanical Design*, Mechanical Engineers' Handbook. New York: John Wiley and Sons, Inc.